

---

# List of publications and presentations

---

## *Paper publications*

1. **Munmi Majumder**, Shibjyoti Debnath, Rahul L. Gajbhiye, Rimpi Saikia, Bhaskarjyoti Gogoi, Suman Kumar Samanta, Deepjyoti K. Das, Kaushik Biswas, Parasuraman Jaisankar, and Rupak Mukhopadhyay. "Ricin *communis* L. fruit extract inhibits migration/invasion, induces apoptosis in breast cancer cells and arrests tumor progression in vivo." *Scientific reports* 9, no. 1 (2019): 1-14. <https://doi.org/10.1038/s41598-019-50769-x>
2. **Munmi Majumder**, Manoj Sharma, Siddhartha Maiti, and Rupak Mukhopadhyay. "Edible tuber *Amorphophallus paeoniifolius* (Dennst.) induces apoptosis and suppresses migration of breast cancer cells *in vitro*." (2020). (under review)

## *Conference presentations*

1. **Munmi Majumder** & Rupak Mukhopadhyay on Influence of two indigenous plant extracts on proliferation, migration, and adhesion of breast cancer cell lines in **International Conference** on Molecular Signaling: Recent Trends in Biosciences organized by Department of Zoology, North-Eastern Hill University, Shillong on 20<sup>th</sup>- 22<sup>nd</sup> November **2015 (Poster)**.
2. **Munmi Majumder** & Rupak Mukhopadhyay on *Ricinus communis* fruit extract inhibits growth and metastasis of breast cancer cell lines MCF-7 and MDA-MB-231 via STAT-3 pathway in **National seminar** on Recent Advances in Medicinal Plants Research of North East India organized by ADP College, Nagaon, Assam on 11<sup>th</sup>- 12<sup>th</sup> November **2016 (Oral)**.
3. **Munmi Majumder** & Rupak Mukhopadhyay on A mechanistic study on the anti-cancer activity of edible tuber *Amorphophallus paeoniifolius* (Dennst) in **National seminar** on Probiotics and Functional Foods on Health Management organized by Department of Food Engineering and Technology, Tezpur University on 04<sup>th</sup>- 05<sup>th</sup> March **2019 (Oral)**.

4. **Munmi Majumder**, Parasuram Jaishankar & Rupak Mukhopadhyay on Fruit extract of a Euphorbiaceae family plant induced apoptosis in breast cancer cells by targeting phosphorylation of STAT3 in a p53 independent manner in **International Conference** on Molecular Basis of Disease & Therapeutics organized by the Central University of Rajasthan, Ajmer on 08<sup>th</sup>- 10<sup>th</sup> November **2019 (Poster)**.

OPEN

# *Ricinus communis* L. fruit extract inhibits migration/invasion, induces apoptosis in breast cancer cells and arrests tumor progression *in vivo*

Munmi Majumder<sup>1</sup>, Shibjyoti Debnath<sup>2</sup>, Rahul L. Gajbhiye<sup>3</sup>, Rimpi Saikia<sup>1</sup>, Bhaskarjyoti Gogoi<sup>4,5</sup>, Suman Kumar Samanta<sup>4</sup>, Deepjyoti K. Das<sup>1</sup>, Kaushik Biswas<sup>2</sup>, Parasuraman Jaisankar<sup>3</sup> & Rupak Mukhopadhyay<sup>1</sup>

Medicinal plant-based therapies can be important for treatment of cancer owing to high efficiency, low cost and minimal side effects. Here, we report the anti-cancer efficacy of *Ricinus communis* L. fruit extract (RCFE) using estrogen positive MCF-7 and highly aggressive, triple negative MDA-MB-231 breast cancer cells. RCFE induced cytotoxicity in these cells in dose and time-dependent manner. It also demonstrated robust anti-metastatic activity as it significantly inhibited migration, adhesion, invasion and expression of matrix metalloproteinases (MMPs) 2 and 9 in both cell lines. Further, flow cytometry analysis suggested RCFE-mediated induction of apoptosis in these cells. This was supported by attenuation of anti-apoptotic Bcl-2, induction of pro-apoptotic Bax and caspase-7 expressions as well as PARP cleavage upon RCFE treatment. RCFE (0.5 mg/Kg body weight) treatment led to significant reduction in tumor volume in 4T1 syngeneic mouse model. HPLC and ESI-MS analysis of active ethyl acetate fraction of RCFE detected four compounds, Ricinine, p-Coumaric acid, Epigallocatechin and Ricinoleic acid. Individually these compounds showed cytotoxic and migration-inhibitory activities. Overall, this study for the first time demonstrates the anti-cancer efficacy of the fruit extract of common castor plant which can be proposed as a potent candidate for the treatment of breast cancer.

Breast cancer is the leading cause of cancer death among women worldwide<sup>1</sup>. The main treatment regimens for breast cancer like surgery, radiation therapy, chemotherapy, targeted hormone therapy are either expensive or have various side-effects<sup>2,3</sup>. So, studies towards finding efficient and cost-effective therapeutic strategies with minimal side effects are important for expansion of current treatment options for breast cancer patients. Medicinal plants are rich sources of bioactive molecules and can be exploited for application as anti-cancer agents. Alkaloids vincristine and vinblastine from the plant *Vinca rosea* and taxol, paclitaxel derived from the plant *Taxus brevifolia* are well established anticancer agents owing to their microtubule-targeting efficacy<sup>4-6</sup>. Podophyllotoxin, a lignin derived from *Podophyllum peltatum* L. or *P. emodi* and their derivatives are also used as anti-cancer drugs in market<sup>7</sup>. While podophyllotoxin act by inhibiting microtubule assembly, its derivatives like etoposides and teniposides act by interacting with DNA and inhibition of DNA topoisomerase II<sup>8</sup>. Camptothecin, a quinoline alkaloid from *Camptotheca acuminata* also acts as commercial anti-cancer drug, which inhibits the DNA enzyme topoisomerase I<sup>9</sup>. Furthermore, purified plant polyphenols, baicalin and fisetin were also shown to possess anti-cancer and apoptosis inducing activity in breast cancer cell lines<sup>10,11</sup>. Curcumin inhibited NF- $\kappa$ B pathway and subsequently, the expression of inflammatory cytokines CXCL-1 and -2, up regulated during metastasis<sup>12</sup>.

<sup>1</sup>Cellular, Molecular and Environmental Biotechnology Laboratory, Department of Molecular Biology and Biotechnology, Tezpur University, Tezpur, 784028, Assam, India. <sup>2</sup>Division of Molecular Medicine, Bose Institute, P1/12 CIT Road, Scheme VIII, Kolkata, 700054, India. <sup>3</sup>Laboratory of Catalysis and Chemical Biology, Organic and Medicinal Chemistry Division, CSIR-Indian Institute of Chemical Biology, Jadavpur, Kolkata, 700032, India. <sup>4</sup>Institute of Advanced Study in Science and Technology Vigyan Path, Paschim Boragaon, Guwahati, Assam, 781035, India. <sup>5</sup>Present address: Department of Biotechnology Royal School of Bio-Sciences Royal Global University Guwahati, Assam, 781035, India. Correspondence and requests for materials should be addressed to R.M. (email: [mrupak@gmail.com](mailto:mrupak@gmail.com))

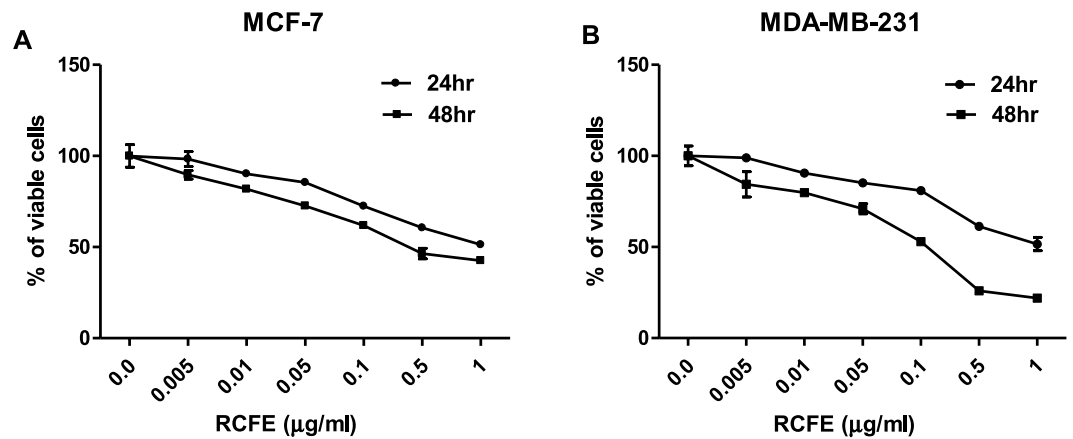


**Figure 1.** RCFE induced cytotoxicity in breast cancer cells. MCF-7 (A) and MDA-MB-231 (B) cells were treated with various concentrations of RCFE for 24 and 48 hr. Data represent the mean  $\pm$  SEM of three independent experiments.

Majority of the breast cancer mortality cases are primarily due to metastasis of the primary cancer to different sites including organs like bones, brain, liver, lymph nodes and lungs<sup>10</sup>. The 5-year survival rate of metastatic breast cancer patients is about 25% suggesting the importance of targeted therapy for metastasis<sup>13,14</sup>. In search of a novel medicinal plant-based therapeutic approach against breast cancer, fruit extract of *Ricinus communis* L. (*Euphorbiaceae*) from North East Indian origin has been studied in detail. North-Eastern part of India is a well-regarded reservoir of traditional medicinal plants as it is one of the prominent biodiversity hotspots of the world<sup>15</sup>. *R. communis* L, commonly known as castor plant, is abundant in North East India and well-known for its traditional and medicinal use globally<sup>16</sup>. In general, various parts of this plant has been used for the treatment of pain, paralysis, constipation, gastritis and warts<sup>17,18</sup>. 50% ethanolic extract of roots of this plants have shown anti-diabetic activity in *in-vivo* rat models<sup>19</sup>. There are other reports which indicate the effectiveness of this plant as anti-fungal agent and also as a pest control measure<sup>19-22</sup>. A volatile extract from the leaves of the plants have shown to induce apoptosis in human melanoma cells (SK-MEL-28)<sup>16</sup>. However, a detailed study on the anti-cancer efficacy of the fruits of *R. communis* L. is not reported.

The current study demonstrates the anti-proliferative activity of *R. communis* L. fruit extract (RCFE) against two breast cancer cell lines MCF-7 and MDA-MB-231. RCFE significantly inhibited migration, adhesion and invasion along with reduction of matrix metalloproteinases 2 and 9 expression. It also induced apoptosis as shown by reduction of anti-apoptotic Bcl-2, induction of pro-apoptotic Bax expression and DNA fragmentation. The induction of apoptosis in both cells was caspase-7 dependent and independent of p53. Interestingly, RCFE inhibited upstream STAT3 activation responsible for induction of MMPs and Bcl-2. RCFE successfully inhibited tumor progression in syngeneic mouse tumor model *in vivo*. HPLC and ESI-MS analysis of the active ethyl acetate fraction of RCFE showed presence of four probable compounds all of which individually showed anti-cancer activities.

## Results

**RCFE induced cytotoxicity in MCF-7 and MDA-MB-231 cells.** To evaluate the cytotoxic effect of RCFE on breast cancer, MCF-7 and MDA-MB-231 cell lines were treated with various concentrations of RCFE for 24 or 48 hr. RCFE treatment significantly increased cytotoxicity in both the cells in dose and time dependent manner (Fig. 1A,B). Treatment with 1 µg/ml RCFE induced cell death by 48.7% and 55.4% in 24 and 48 hr incubation, respectively in MCF-7 cells (Fig. 1A). Treatment with same concentration led to 48.4% and 78.5% cell death in MDA-MB-231 cells at these time points, respectively (Fig. 1B). To understand the cytotoxic specificity of RCFE, additional cell lines of cancer and normal origin were treated with the extract. Amongst these, HER2-positive MDA-MB-453 and triple-positive ZR-75-1 breast cancer cells showed 36.2% and 54.3% cell death when treated with 1 µg/ml RCFE for 48 hr (Supplementary Fig S1). Similar treatment showed significant cytotoxicity in colon cancer cell line HT-29 (64%) and adenocarcinoma cell line A549 (54.2%) after 48 hr (Supplementary Fig S1). In contrast, treatment with similar doses of RCFE showed minimal effect on the HEK293 and mouse embryonic fibroblast (MEF) cells suggesting the extract's cytotoxic specificity against cancer cells (Supplementary Fig S1).

**Inhibition of migration, adhesion and invasion of MCF-7 and MDA-MB-231 cells by RCFE.** As migration is a primary step in cancer metastasis, we studied the effect of RCFE on migration of MCF-7 and MDA-MB-231 cells using wound healing assay. Near-confluent monolayer of cells was pre-treated with Mitomycin C (1 µg/ml) to confirm the wound healing was due to cell migration and not due to proliferation. RCFE treatment for 24 and 48 hr demonstrated dose-dependent inhibition of migration in both cells (Fig. 2A,B). The inhibition of migration in response to 0.05 µg/ml of RCFE after 24 hr was not significant in MCF-7 cells. However, the same concentration was sufficient to inhibit migration significantly after 48 hr. The effect was highly significant when MCF-7 cells were treated with higher concentration of RCFE (0.1 µg/ml) even at 24 hr. Interestingly, the effect of RCFE on inhibition of migration was robust on highly metastatic MDA-MB-231

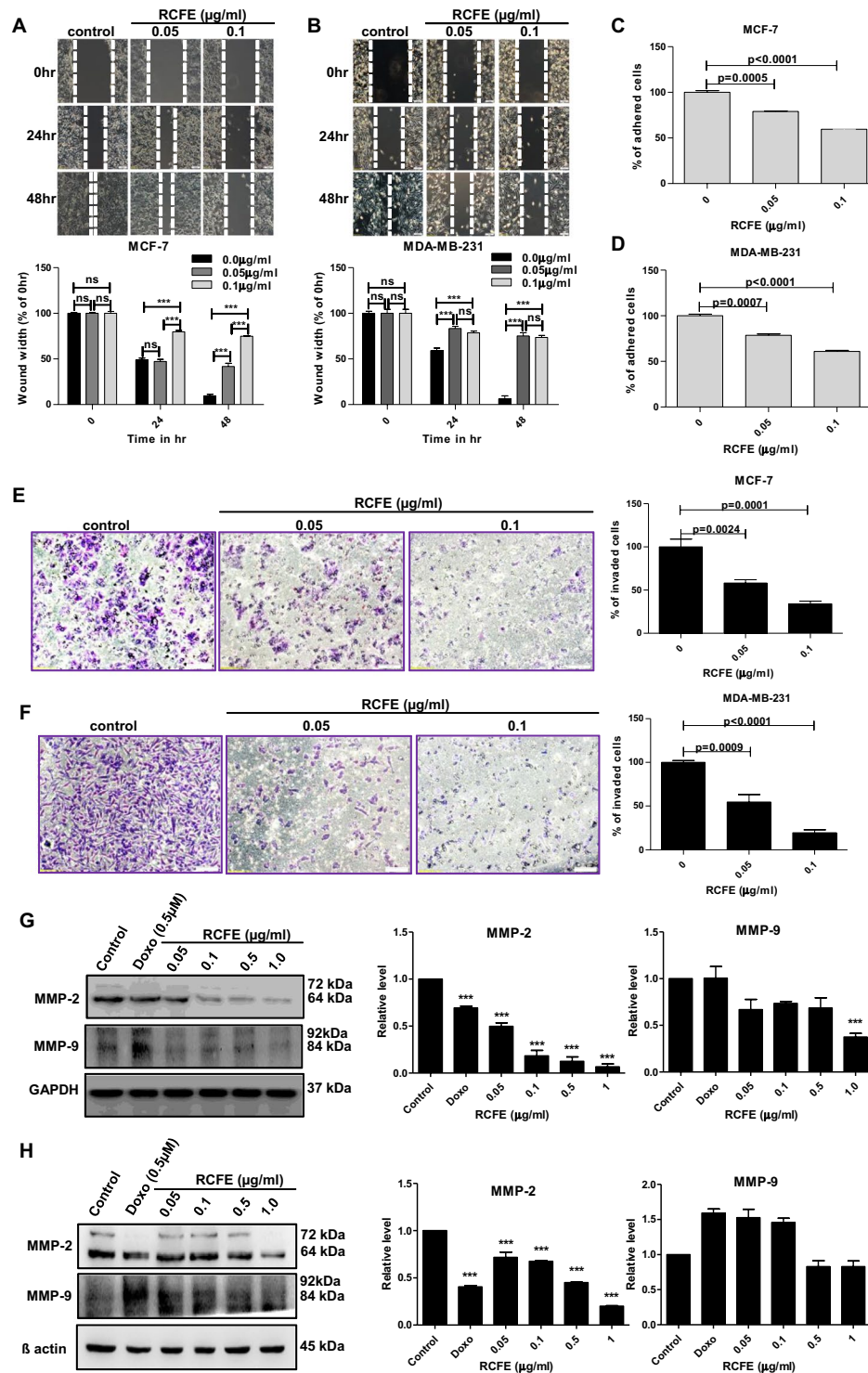


**Figure 2.** RCFE inhibited metastatic properties of breast cancer cells. Inhibition of migration of MCF-7 (A) and MDA-MB-231 (B) with treatment of 0.05 and 0.1  $\mu\text{g/ml}$  for 24 and 48 hr. The quantification of wound widths was shown in right panels. Data represent the mean  $\pm$  SEM of three independent experiments. Statistical differences were analyzed with two-way ANOVA test. p value ns > 0.05, p value \*\*\* < 0.0001. Effect of RCFE on adhesion of MCF-7 (C) and MDA-MB-231 (D). Data represented as mean  $\pm$  SEM of three independent experiments. Statistical differences were analyzed with one-way ANOVA test. p value < 0.05 was considered significant. Invasion of MCF-7 (E) and MDA-MB-231 (F) cells through ECM gel coated transwell inserts in response to RCFE. Data represent the mean  $\pm$  SEM of five different images of individual set of three independent experiments (shown in right panels). Statistical differences were analyzed with student t-test. p value < 0.05 was considered significant. Western blot analysis of MMP-2 and -9 in MCF-7 (G) and MDA-MB-231 (H) cells in response to treatment with RCFE. The quantitation of band intensities was represented in bottom panels. Statistical differences were analyzed with one-way ANOVA test. p value < 0.05 was considered significant.

as shown by significant inhibition of migration in these cells after treatment with both the doses for 24 and 48 hr (Fig. 2B). Ability to adhere to extracellular matrices is one of the hallmarks of metastatic cancer cells. Pre-treatment of both MCF-7 and MDA-MB-231 cells with two concentrations of RCFE demonstrated significant reduction in adhesion of the cells to collagen IV coated wells in a dose-dependent fashion (Fig. 2C,D). Treatment with 0.05 µg/ml and 0.1 µg/ml RCFE inhibited adherence by 21% and 41% in MCF-7 cells and 22% and 40% in MDA-MB-231 cells, respectively.

Further, the effect of RCFE on invasion of two breast cancer cells was studied. Cells pre-treated with or without RCFE were allowed to invade through extracellular matrix (ECM) gels in response to 10% FBS-containing medium. In MCF-7 cells, treatment with 0.05 and 0.1 µg/ml of RCFE reduced 42% and 66% invasion compared to control cells (Fig. 2E). Interestingly again, the effect was more prominent in MDA-MB-231 cells as treatment with these two concentrations of RCFE led to 45% and 81% reduction in invasion after 6 hr (Fig. 2F).

As these experiments pointed towards anti-metastatic role of RCFE, the expression of metastasis-associated matrix metalloproteinase 2 and 9 (MMP-2 and 9) were studied next. Western blot analysis suggested treatment of RCFE for 24 hr reduced expression of MMP-2 and MMP-9 in MCF-7 and MDA-MB-231 cells in concentration-dependent manner (Fig. 2G,H). RCFE at a concentration of 1.0 µg/ml reduced the MMP-2 expression by about 10 folds in MCF-7 cells and 4 folds in MDA-MB-231 cells. Treatment with the same concentration of RCFE led to ~ 2 folds reduction in expression of MMP-9 in both the cells.

**RCFE induced apoptosis in MCF-7 and MDA-MB-231 cells.** Since, apoptosis is a plausible mode of controlling cancer cell proliferation by an anti-cancer agent; we next studied the role of RCFE in inducing apoptosis in two cell lines. Flow cytometric analysis was performed with cells treated with 0.5 and 1.0 µg/ml RCFE for 24 hr (Fig. 3A,B). In MCF-7 cells, both treatments induced more than 3 folds augmentation in apoptosis (early and late). The increase in apoptosis in MDA-MB-231 cells were found to be 2.7 folds (0.5 µg/ml) and 11 folds (1.0 µg/ml), respectively. Genomic DNA isolated from the cells following treatment with 1.0 µg/ml RCFE for 24 and 48 hr showed degradation of DNA (Supplementary Fig S2).

To understand the signaling mechanism leading to RCFE-induced apoptosis in MCF-7 and MDA-MB-231 cells, expression level of apoptosis regulating proteins like Bax, Bcl-2, PARP, and Caspase-7 were assessed by western blot (Fig. 3C,D). Treatment with RCFE augmented expression of apoptotic protein Bax and concomitantly inhibited anti-apoptotic protein Bcl-2 expression in a concentration-dependent manner in both the experimental cells. This led to increase in Bax/Bcl-2 ratio, critical for cells undergoing apoptosis (Right panels; Fig. 3C,D). Bcl-2 inhibition leads to release of cytochrome c from the mitochondrion which induces the caspase pathway. Treatment with RCFE increased expression level of caspase-7 in dose-dependent manner suggesting onset of apoptosis in the cells (Fig. 3C,D). Significant increase in caspase-7 level was found in cells treated with higher concentrations of RCFE (Right panels; Fig. 3C,D). PARP, a DNA repair enzyme, is a substrate of caspases and increase in PARP cleavage indicates apoptosis in the cells. PARP cleavage as a result of RCFE treatment confirmed caspase-mediated apoptosis in both MCF-7 and MDA-MB-231 cells (Fig. 3C,D). Doxorubicin (0.5 µM) was used as positive control in this study. To understand if cell cycle arrest was also involved in anti-cancer activity of RCFE, expression of Cyclin E1 was studied. In both MCF-7 and MDA-MB-231 cells, the expression of Cyclin E1 did not change significantly with increased concentration of RCFE suggesting cells were not arrested in G1/S phase (Supplementary Fig S3). Expression of tumor suppressor gene p53 was also studied as activation of p53 was proposed to play key role in cell cycle arrest and apoptosis<sup>23</sup>. Treatment with RCFE did not show any activation of p53 in the cells suggesting the RCFE-induced apoptosis in these cells was primarily independent of p53 (Supplementary Fig S3).

**RCFE inhibited phosphorylation of STAT3.** JAK-STAT pathway is involved in activation of proteins related to apoptosis and metastasis including Bcl-2 and MMP2/9. We investigated the status of STAT3 phosphorylation in these cells followed by RCFE treatment. Treatment with increasing concentration of RCFE significantly reduced phosphorylation at Tyr705 of STAT3, without alteration of total STAT3 protein level (Fig. 4A,B). The reduction in STAT3 phosphorylation was more evident in MCF-7 cells as treatment with 1 µg/ml RCFE almost abolished the phosphorylation. All the above observations pointed towards coordinated role of RCFE in induction of apoptosis and reduction of metastasis in breast cancer cells (represented as a model in Fig. 4C).

**RCFE inhibited tumor growth in syngeneic mouse model.** To understand the effect of RCFE on progression of *in vivo* breast tumor, transplantable mouse mammary carcinoma 4T1 cell induced model was studied. RCFE showed significant cytotoxicity against these cells *in vitro* as shown in Fig. 5A. Tumor was induced in female Balb/c mouse by subcutaneous injection of 4T1 cells in mammary fat pad. After 10 days, intraperitoneal administration of 4 doses of RCFE (at 0.5 mg/kg bodyweight concentration) were given to one set of animals, while the other set of animals received only vehicle (0.9% saline). The tumor continued to increase in the control group while RCFE treated animals showed significant reduction in tumor volume with time (Fig. 5B). The resected tumors from the sacrificed animals at 22 days following 4T1 injection are shown in Fig. 5B (lower panel). RCFE-treated animals showed more than 88% reduction tumor volumes compared to control group animals (Fig. 5C).

**Identification of bioactive components in RCFE.** To identify bioactive components of RCFE, the dried hydro-ethanolic extract was successively fractionated into ethyl acetate, butanol and aqueous fractions. The cytotoxic activity of these fractions was studied which suggested comparatively higher activity in ethyl acetate fraction (Supplementary Fig S4). Hence, this fraction was subjected to HPLC finger printing analysis. Four characteristic peaks were identified in the RP-HPLC analysis (Fig. 6A,B). Retention time, name, molecular formula, molecular weight and chemical structure of the components are shown in Table 1. The major peaks eluted after HPLC was

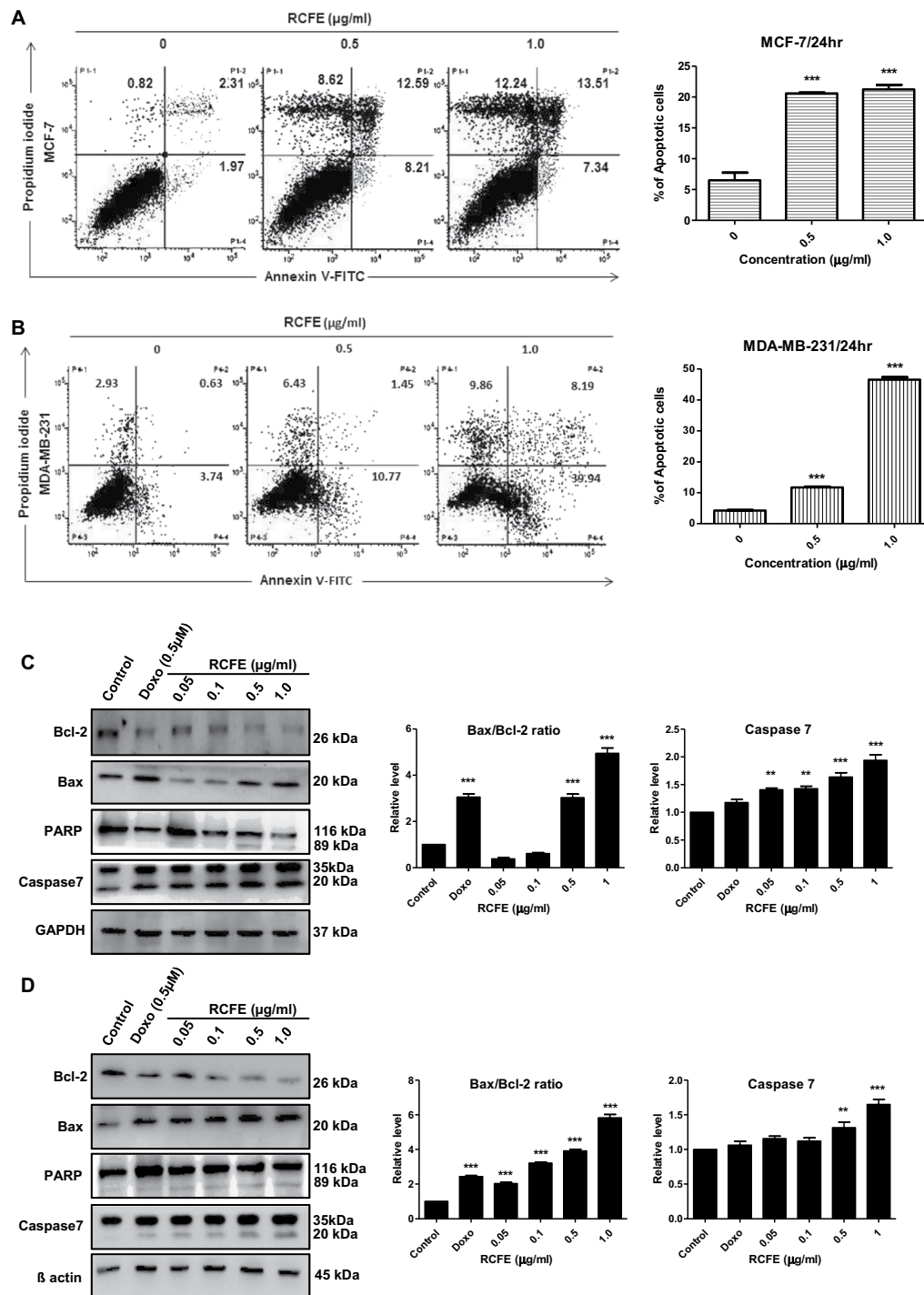


**Figure 3.** Induction of apoptosis by RCFE. Flow cytometer analysis of MCF-7 (**A**) and MDA-MB-231 (**B**) using Annexin V/PI. The quantitation of three independent analysis was presented in right panels. Western blot analysis of lysates from MCF-7 (**C**) and MDA-MB-231 (**D**) with antibodies against Bcl-2, Bax, PARP and Caspase-7. The ratio of Bax/Bcl-2 and caspase-7 expressions were normalized either to GAPDH or  $\beta$ -actin presented in the right panels. Doxorubicin (Doxo) was used as positive control. Statistical differences were analyzed with one-way ANOVA test. p value < 0.05 was considered significant.

collected, evaporated and their ESI-MS was recorded (Fig. 6C–F). The probable compounds peaks were recognized as Ricinine<sup>24</sup>, p-Coumaric acid<sup>25</sup>, Epigallocatechin<sup>26</sup> and Ricinoleic acid<sup>25</sup> by comparing ESI-MS spectra with previously reported literature (Table 1).

**Cytotoxicity and migration inhibitory activity of pure compounds.** To evaluate the cytotoxicity of four compounds identified from RCFE, MCF-7 and MDA-MB-231 cell lines were treated with increasing

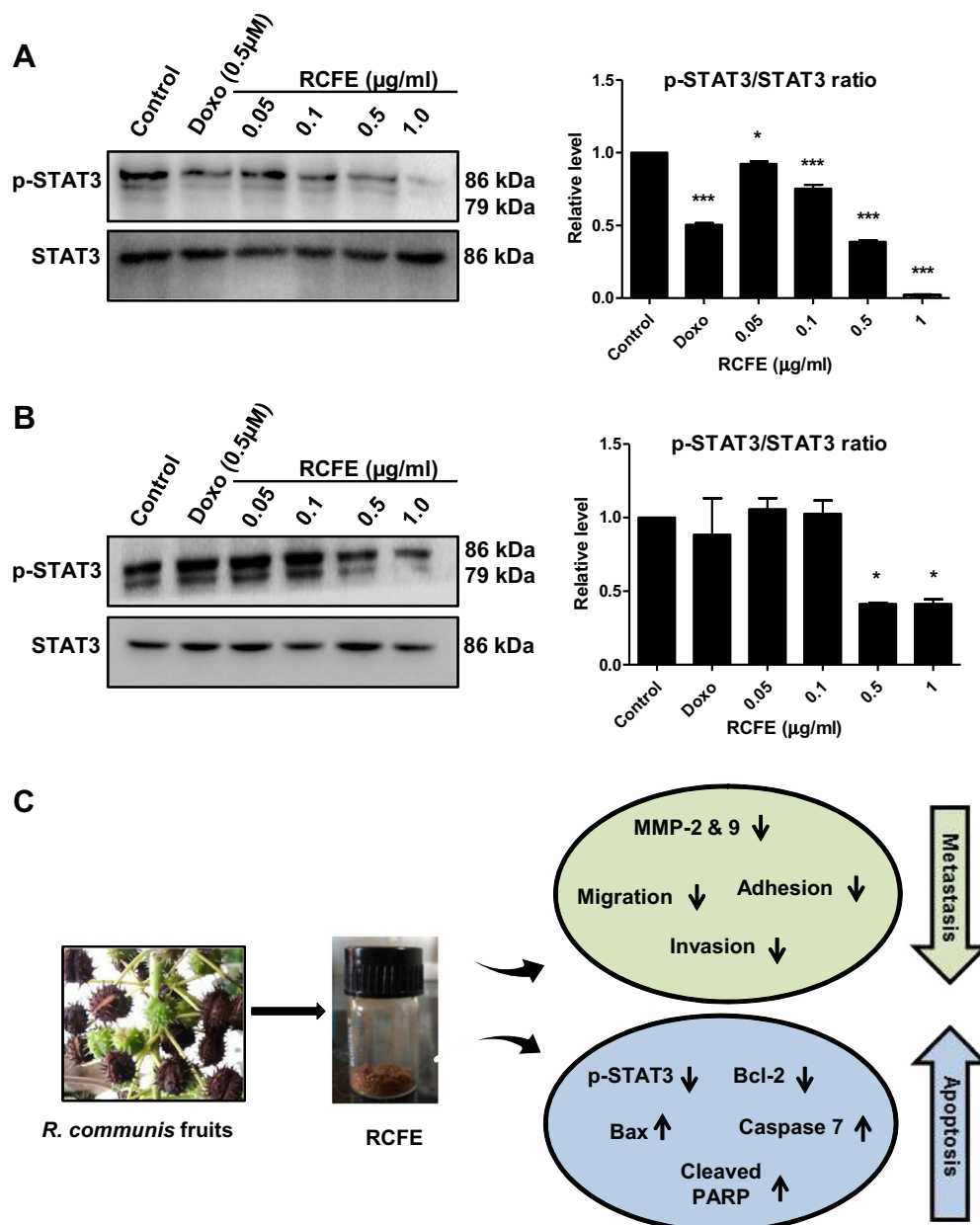


**Figure 4.** RCFE treatment led to inhibition of STAT3 phosphorylation. Western blot analysis of MCF-7 (A) and MDA-MB-231 (B) cell lysates with phosphor-STAT3 (Tyr705) and STAT3 antibodies. The quantitation of the expression was presented in right panels. Doxorubicin (Doxo) was used as positive control. Statistical differences of three independent experiments were analyzed with one-way ANOVA test.  $p$  value  $< 0.05$  was considered significant. (C) Schematic representation of the metastasis inhibition and apoptosis induction by RCFE for its anti-cancer activity.

concentrations of the Ricinine, p-Courmaric acid, Epigallocatechin and Ricinoleic acid for 24 hr. All four compounds showed cytotoxicity against both cells in a dose dependent manner (Fig. 7A). However, our data suggested that, Ricinine, p-Courmaric acid and Ricinoleic acid were more effective against MDA-MB-231 cells, while Epigallocatechin showed better cytotoxic effect against MCF-7.

Next, the effect of these compounds on migration of MCF-7 and MDA-MB-231 cells was studied using wound healing assay (Supplementary Fig S5). The inhibition of MCF-7 cell migration was not significant for the compounds after 24 hr of treatment with two concentrations of 10 and 20 µM (Fig. 7B). However, the effect was more prominent after 48 hr of treatment which showed inhibition of MCF-7 migration by Ricinine, Epigallocatechin and Ricinoleic acid. The scenario was different in MDA-MB-231 cells where Ricinine and p-Courmaric acid showed no effect after 24 hr treatment and moderate effect after 48 hr (Fig. 7C). Interestingly, Epigallocatechin treatment strongly inhibited MDA-MB-231 cell migration in a dose and time-dependent manner (Fig. 7C). The inhibitory effect of Ricinoleic acid on migration of MDA-MB-231 cells was also highly significant after 48 hr of treatment.



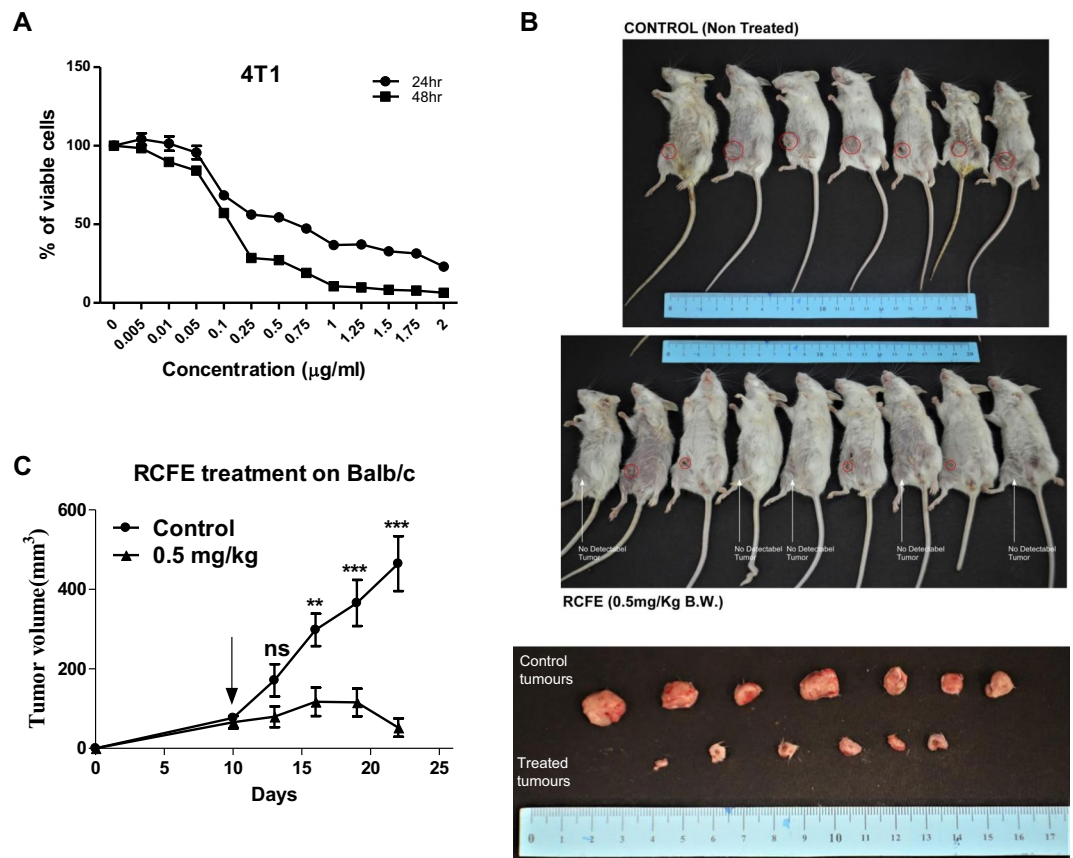
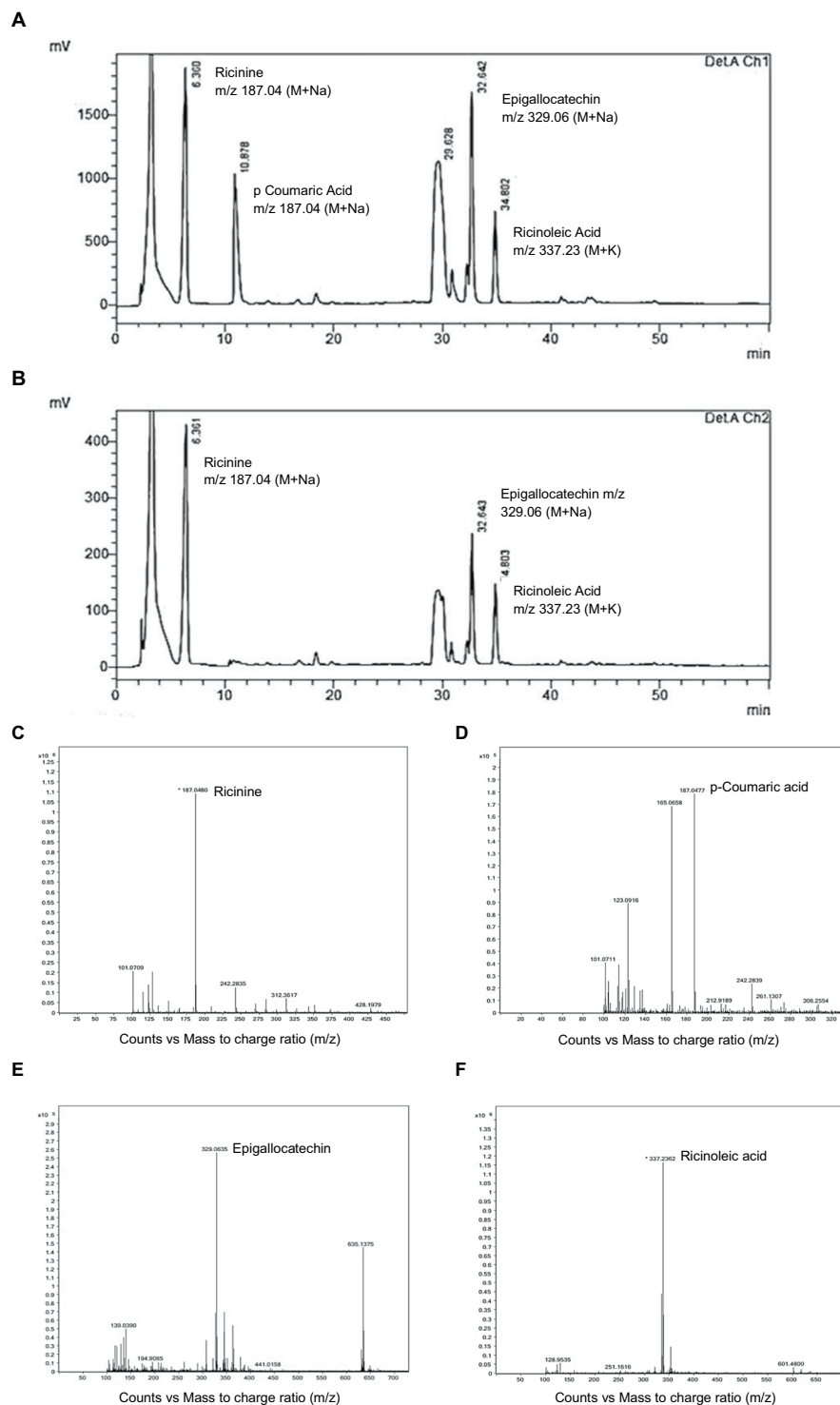


**Figure 5.** RCFE inhibited tumor progression: (A) 4T1 cells were treated with various concentrations of RCFE for 24 and 48 hr. Data represent the mean  $\pm$  SEM of three independent experiments. (B) The animals treated with 0.9% normal saline (upper panel) and RCFE at 0.5 mg/kg bodyweight (middle panel). Animals with visible tumor from outside was pointed with red circles. Animals with no visible tumors from outside was shown by white arrows. The excised tumors from control and RCFE-treated animals (bottom panel). (C) Graph represented the measured tumor volumes in two different treatments. Statistical differences were analyzed with two-way ANOVA test. p value ns  $>$  0.05, p value \*\*\*  $<$  0.0001.

## Discussion

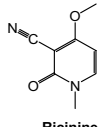
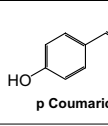
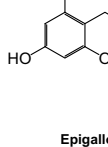
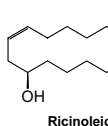
It is now well documented that medicinal plants are a ‘treasure trove’ of bioactive molecules for the treatment of various human diseases. In the last few decades, numerous traditional knowledge-based drugs have been isolated and commercialized<sup>27–29</sup>. Multiple molecules of medicinal plant origin are currently used as drugs to combat cancer (e.g. vincristine, vinblastine, taxol, paclitaxel, Podophyllotoxin). The current study reports the mechanistic details of anti-cancer activities of the fruit extract of *Ricinus communis* L. (RCFE), commonly known as castor bean plant. Oil and seeds of this plant are widely used in folk medicine as purgative, against worm infestation and arthritis. It has also been reported to have anti-inflammatory effects. However, there are no detailed reports on the mechanism of anti-cancer efficacy of this plant.

Metastasis, the property that empowers certain cancer cells to spread into local or distant tissues is a complex process involving migration, adhesion and invasion. These processes can be targeted by an anti-metastatic agent leading to attenuated aggression of cancer cells. Migration of cancer cells to different tissues is an important initial step in metastasis. Treatment with RCFE inhibited migration of both MCF-7 and MDA-MB-231 in a dose-dependent manner. Initiation of metastasis also depends on adhesion property of the cells that involves interaction with extracellular matrix following detachment from the primary sites. RCFE at very low concentrations significantly inhibited adhesion of cells with collagen IV which is an integral part of the basement membrane<sup>30</sup>. The process of invasion is critical for metastasis because the motile cells need to cross the extracellular matrix and spread into surrounding tissues<sup>31</sup>. In this study, RCFE substantially inhibited efficacy of the cells to invade ECM gel to reach other side of the insert in response to a media containing 10% FBS. The highest inhibition of invasion (81%) was achieved in MDA-MB-231 cells after treatment with a very low concentration of 0.1  $\mu\text{g/ml}$  of RCFE for 24 hr. Remarkably, RCFE showed greater inhibition of cell migration and invasion in highly aggressive triple negative MDA-MB-231 cells compared to MCF-7 cells suggesting its probable application to manage highly aggressive cancer cells. The process of invasion and metastasis is accompanied with degradation of connective tissues and as a result expression of matrix degrading enzymes e.g. matrix metalloproteinases (MMPs) increases. MMP-2 and 9 have been shown to overexpress and contribute to metastatic efficacy of MDA-MB-231<sup>30</sup>. Here, we showed that expression of MMP-2 and 9 were inhibited by RCFE emphasizing its effect on ECM degradation and invasion of cancer cells.



**Figure 6.** Fingerprint analysis of ethyl-acetate fraction of RCFE. RP-HPLC chromatogram of the ethyl-acetate fraction at a wavelength of (A) 210 nm (Det A Ch1) and (B) 254 nm (Det B Ch2). ESI-MS spectra of fractions collected after RP-HPLC were identified as Ricinine (C), p-Coumaric acid (D), Epigallocatechin (E) and Ricinoleic acid (F).

We studied the mechanism of RCFE-induced cell death in MCF-7 and MDA-MB-231 cells. Cell death in these cells via apoptosis was confirmed by flow cytometry analysis using Annexin V/PI. It is clear from the analysis that, RCFE induced apoptosis in a significant percentage of cells. DNA fragmentation assay, a widely used biochemical marker of apoptosis, was performed to confirm this observation. DNA fragmentation occurs at the inter-nucleosomal linker regions in the cells undergoing apoptosis<sup>32–34</sup>. To elucidate the mechanism of apoptosis expression of several pro and anti-apoptotic proteins was studied. RCFE inhibited the expression of

Peak No.	$t_R$ (min)	Comparative Area%	m/z ( $M^+$ )	m/z ( $M + Na$ )	m/z ( $M + K$ )	Molecular Formula	Compound name & Structure	Reference
1	6.36	26.015	164	187.04	—	$C_8H_8N_2O_2$	 Ricinine	Wachira <i>et al.</i> <sup>24</sup>
2	10.87	14.387	164	187.04	—	$C_9H_8O_3$	 p Coumaric Acid	Wafa <i>et al.</i> <sup>25</sup>
3	32.64	14.499	306	329.06	—	$C_{15}H_{14}O_7$	 Epigallocatechin	Singh <i>et al.</i> <sup>26</sup>
4	34.80	7.661	298	—	337.23	$C_{18}H_{34}O_3$	 Ricinoleic Acid	Wafa <i>et al.</i> <sup>25</sup>

**Table 1.** Probable compounds identified by HPLC and ESI-MS technique.

anti-apoptotic protein Bcl-2 and induced the expression of pro-apoptotic protein Bax. Expression of Bcl-2 and Bax family proteins plays significant role in the decision of inducing apoptosis in a cell by altering the release of cytochrome c from mitochondria by regulating mitochondrial membrane permeability<sup>35</sup>. Inhibition of Bcl-2 by RCFE possibly induces the cytochrome c production that leads to expression of caspases. Caspases are the key players of apoptosis and a variety of caspases are involved in intrinsic, extrinsic and execution of apoptotic pathway<sup>35</sup>. Caspases use PARP as substrate and cleave PARP during apoptosis<sup>35–37</sup>. We found one of the family members, Caspase 7, a major caspase involved in execution pathway was up regulated in both MCF-7 and MDA-MB-231 validating its role in inducing apoptosis in response to RCFE treatment. Further, increased PARP cleavage with treatment of increasing concentration of RCFE confirmed apoptosis inducing activity of the extract. Expression of p53, a key factor known to induce apoptosis, did not increase suggesting the minimal effect of p53 in inducing apoptosis by treatment of RCFE.

Attenuation of metastasis and induction of apoptosis by RCFE might be attributed to its activity to down regulate phosphorylation of STAT3, a master regulator for these two pathways in cancer cells. Aberrant JAK-STAT signaling (specifically STAT3) is common in various cancer due to their constitutive activation in response to stimulators e.g. cytokines, growth factors, receptors (TLRs/GPCRs), polypeptide ligands and miRNAs<sup>38</sup>. STAT3 induces expression of MMPs and promotes invasion and metastasis in cancer cells. In addition, it induces anti-apoptotic Bcl-2 expression leading to survival of the cells. So, targeting STAT3 has been suggested as a viable therapeutic strategy against cancer<sup>38</sup>. RCFE mediated deactivation of Tyr705 phosphorylation of STAT3 inhibited these two critical steps leading to attenuation of metastatic and induction of apoptosis suggesting possible application of this extract against breast cancer therapy.

The anti-cancer efficacy of RCFE was highlighted by the 4T1 syngeneic mouse model. 4T1 cells are highly tumorigenic and thus suitable for generation of mammary tumors in animals with characters close to human mammary tumors<sup>39</sup>. Our data suggested that 4 doses of intraperitoneal administrations of RCFE at a concentration as low as 0.5 mg/kg bodyweight reduced the tumor volume by about 88% emphasizing its role in limiting breast tumors *in vivo*. Several animal models are reported to study efficacy of drugs against breast cancer: xenograft, genetically engineered (transgenic) and syngeneic models being the most common of them. While xenograft models are popular as it mimics human tumors, it eliminates the possibility of immune response against the tumor leading to host-tumor interaction unnatural to human tumor development<sup>40</sup>. Transgenic animal models overcome this problem and can be used to screen drugs against tumorigenesis. However, genetic changes should be tissue specific in these models, as oncogene-bearing or tumor suppressor gene-knock out systemically may not imitate tumors arising out of mutations in normal microenvironment<sup>40</sup>. These models also take several months to generate tumor and are expensive. Syngeneic models, on contrary, are simple and inexpensive model. Murine adenocarcinoma 4T1 cells implanted in immunocompetent Balb/c, as used in this study, is the most widely used syngeneic model to study tumor progression and metastasis<sup>41</sup>. In future we would like to use this model to understand the efficacy of RCFE to reduce tumor volume through host immune modulation, which would be the subject and focus of an entirely independent study. It would also be interesting to know if the extract would regulate 4T1 cells-induced metastasis in these animals and map the metastatic signaling pathways that might be modulated upon RCFE treatment. We plan to study these aspects in detail to confirm *in vivo* anti-metastatic activity of RCFE.

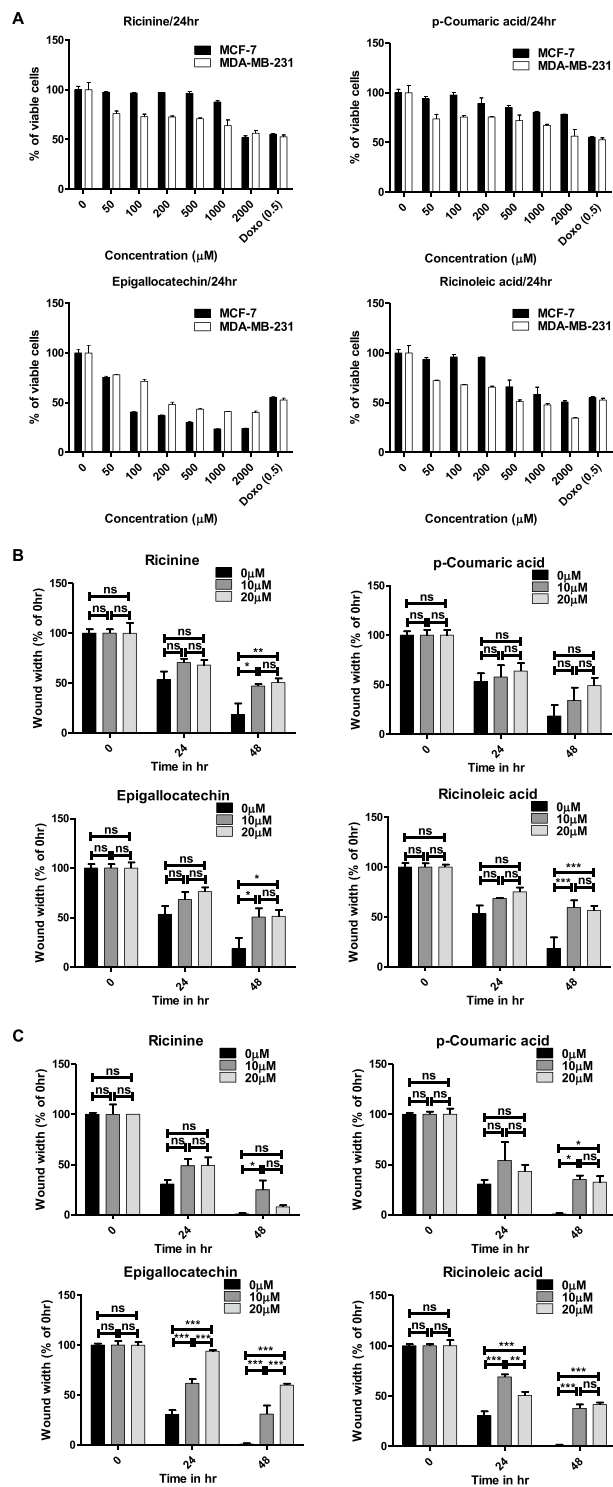


**Figure 7.** Pure compounds showed significant biological activity. (A) The cytotoxic effect of Ricinine, p-Coumaric acid, Epigallocatechin and Ricinoleic acid in MCF-7 and MDA-MB-231 cells after 24 hr treatment. Doxorubicin (Doxo) was used as positive control. Quantitative representation of migration of MCF-7 (B) and MDA-MB-231 (C) cells by wound healing assay. Data represent the mean  $\pm$  SEM of three independent experiments. Statistical differences were analyzed with two-way ANOVA test for wound healing assay. p value  $ns > 0.05$ , p value  $*** < 0.0001$ .

It is important to have knowledge about constituent molecule(s) of a bioactive plant extract for its probable use as therapy. We performed HPLC and ESI-MS analysis of the ethyl acetate fraction of the extract which revealed the presence of four individual compounds namely, Ricinine, p-Coumaric acid, Epigallocatechin and

Ricinoleic Acid. Of them, Ricinine and Ricinoleic Acid have not been reported for any anti-cancer activity albeit their prominent pharmacological importance<sup>42–44</sup>. However, p-Coumaric acid, a hydroxy derivative of cinnamic acid was shown to inhibit proliferation of colon cancer cells in dose-dependent manner<sup>45</sup>. It induced apoptosis accompanied with increasing reactive oxygen species (ROS) levels, a fall in the mitochondrial membrane potential and increased lipid layer breaks. Ethanolic extract of Chinese propolis, where p-Coumaric acid is one of the components, exert antitumor effects mainly through inducing apoptosis of breast cancer cells<sup>46</sup>. Furthermore, Epigallocatechin was also reported for inducing apoptosis and cell cycle arrest<sup>47</sup>. We studied the cytotoxic and migration-inhibitory efficacy of all four compounds to have insight on their individual roles as anti-cancer molecules. Though all four compounds showed cytotoxicity, their efficacy varied with cell types. The inhibition of migration in MCF-7 cells was possibly due to combination of Ricinine, Epigallocatechin and Ricinoleic acid as effect of p-coumaric acid was found to be nominal. Interestingly, in highly metastatic MDA-MB-231 cells, Epigallocatechin contributed most significantly in abrogating migration. However, Ricinoleic acid and Ricinine also contributed moderately to inhibit migration in MDA-MB-231 cells. It may be assumed that the anti-cancer efficacy of RCFE is contributed by synergistic effect of either the identified compounds or their combination with some unidentified compounds.

In summary, our study demonstrated the efficacy of the fruit extract of common castor plant *R. communis* L. against two breast cancer cells of distinctive characteristics. The extract inhibited aggressiveness of the cancer cells by inhibiting characters of metastasis such as cell motility, adhesion, invasion and reduced MMP-2 and 9 expressions. Treatment with the extract induced apoptosis in the cells by augmenting Bax/Bcl-2 ratio that is known to induce caspases and subsequent cleavage of PARP. The phosphorylation of STAT3, a central regulator for activation of metastasis and anti-apoptotic molecules, was inhibited by the extract. The extract significantly reduced tumor volumes in 4T1 syngeneic mouse model. HPLC fingerprinting along with ESI-MS analysis suggested presence of four compounds, all of which showed anti-cancer efficacy individually. The current report contributes significantly to the repertoire of plant-derived therapeutic strategies for the treatment of breast cancer. In future, it would be interesting to study the extract's role in inhibiting metastasis and modulating immune response for tumor reduction in suitable animal model.

## Methods

**Cell lines and reagents.** The cell lines MCF-7, MDA-MB-231, MDA-MB-453, ZR-75-1, HT-29, A549 and HEK293 were purchased from NCCS Pune, India. MEF was a gift from Dr. Sougata Saha, Tezpur University, India. DMEM (Dulbecco's Modified Eagle Medium) and FBS (Fetal Bovine Serum) were purchased from Life Technologies, USA. MTT (3-(4, 5-dimethylthiazolyl-2)-2, 5-diphenyltetrazolium bromide), Collagen IV, ECM gel and Doxorubicin were also purchased from Sigma Aldrich and Mitomycin C was purchased from HiMedia, India. Annexin-V-FLUOS Staining Kit purchased from Roche, USA and Annexin V FITC Assay Kit was purchased from Cayman, USA. Antibodies used in this study were procured from Cell Signalling Technology, USA.

**Preparation of extracts.** Fresh fruits of the plant *Ricinus communis* L. were collected from the Golaghat district of the state of Assam in North East India and morphological identification of the specimen were done at the Botanical Survey of India, Shillong, Meghalaya. The dried fruits were extracted with 50% denatured ethanol at room temperature for 48 hr each time. The extract was filtered and then concentrated under reduced pressure to remove excess ethanol and finally was lyophilised to obtain ethanolic extract (named RCFE). A part of RCFE (5 gm) was then suspended in sterile de-ionised water and partitioned successively with ethyl acetate and n-Butanol. Each fraction was evaporated under vacuum and lyophilized to yield the EtOAc [RC(E)], n-BuOH [RC(B)] and aqueous [RC(A)] fractions. All the fractions were stored at 4 °C and checked for the biological activity.

**Cell culture.** MCF-7, MDA-MB-231, MDA-MB-453, HT-29, A549, MEF and HEK293 cell lines were routinely maintained in Dulbecco's modified Eagle's medium (DMEM; Gibco), and ZR-75-1 in RPMI1640 supplemented with 10% fetal bovine serum and 1% antibiotic. Cell lines were kept in a CO<sub>2</sub> incubator at 5% CO<sub>2</sub> and 37° C temperatures.

**Cytotoxicity assay.** In this assay, cells (5000 each) were plated in a 96 well plate and incubated for 48 hr. Cells were treated with different concentrations of RCFE up to 48 hr. Following incubation, cells were treated with MTT and incubated for 3.5 hr. The media was removed carefully and MTT dissolving solution was added and absorbance was taken at 590 nm wavelength using UV-Vis spectrophotometer (Multiscan Go, ThermoScientific).

**Migration assay.** Cells were seeded in a 24 well plate till 90% confluency. The media was replaced by FBS-devoid media for at least 6 hr and mitomycin C (1 µg/ml) was added before 1 hr of treatment to stop proliferation. Using a sterile pipette tip, a straight scratch was made simulating a wound in each of the wells. The extract at various concentrations were added and images were taken at 0, 24 and 48 hr following the treatment from at least 3 different fields of each well. The width of the wound was measured and quantified.

**Adhesion assay.** To evaluate the efficacy of the extracts to inhibit adhesion,  $2 \times 10^5$  cells/ml were pre-treated with different doses of extracts in serum free media for 24 hr. Cells were then plated in 96-well plates pre-coated with collagen IV and allowed to adhere for 60 min. The media was gently removed, and the wells were washed. The attached cells were quantified using MTT.

**Invasion assay.**  $2.5 \times 10^5$  cells/well were plated in a 6 well plate with or without treatment in a serum free media for 24 hr. Then cells were trypsinised and resuspended in 200 µl serum-free media and placed in the upper chamber of ECM gel pre-coated transwell inserts. The lower chamber was filled with 10% FBS containing media

to create a concentration gradient and incubated for 24 hr in case of MCF-7 and 6 hr in case of MDA-MB-231. Then inserts were washed and cells were fixed with formaldehyde and permeabilized with methanol. The cells were then stained with Giemsa stain. Non-invasive cells were removed by scrapping with a cotton swab and bright field images of invasive cells were taken using Olympus IX83 microscope. The cells were counted from photomicrographs of 10 random fields of a single membrane.

**DNA fragmentation assay.** Both MCF-7 and MDA-MB-231 cells were treated with RCFE (1 µg/ml) for 0, 24 and 48 hr. Cells were trypsinised and genomic DNA was isolated using PureLink™ Genomic DNA Mini Kit (Invitrogen, USA). Concentration was measured, and DNA was run on 2% agarose gel.

**Flow cytometer analysis.** MCF-7 and MDA-MB-231 cells ( $1 \times 10^5$  cells/well) were seeded in 12 well culture plates and incubated for overnight. Then adhered cells were treated with RCFE 0.5 µg/ml and 1 µg/ml for 24 hr. No treatment was given to the control cells. After incubation, both floating as well as adherent cells from each well were collected in tubes and washed with PBS. The cell pellets were resuspended in 200 µL of binding buffer and required proportions of FITC-Annexin V/PI were added to each sample according to manufacturer's protocol of Annexin V FITC Assay Kit (Cayman, USA). The samples were then allowed to incubate in dark for 15 min and then analyzed with FACSCorus software on a FACS Melody flow cytometer (BD Biosciences).

**Western blot analysis.** Cells were seeded in 100 mm dish at  $1 \times 10^6$  cells per dish and incubated overnight before treating with the indicated concentrations for 24 hr. Proteins were extracted from RCFE treated MCF-7 and MDA-MB-231 cells with ice cold RIPA buffer (Thermo Scientific, USA) containing protease and phosphatase inhibitor cocktail (Thermo Scientific, USA). Equal amount of proteins from different experimental samples was run in SDS-PAGE and proteins were transferred to a PVDF membrane using semidry electrophoresis transfer unit (GE Healthcare, UK). After blocking with 3% BSA in TBS-Tween 20 for at least 1 hr at room temperature, the membranes were probed with the corresponding primary antibody (1:1000 dilutions) overnight at 4 °C and secondary antibodies for 1 hr at room temperature. The blots were then incubated with chemiluminescence substrate (Bio-Rad, USA) and bands were visualized using Chemidoc XRS+ system (Bio-Rad, USA). Quantification of the bands was done using Gel Quant software.

**In vivo study of mouse tumor model.** Female Balb/c mice 6–8-week-old were obtained from Center for Translational Animal Research (CTAR), Bose Institute, Kolkata, India and were maintained as per the guidelines of the animal ethical committee in accordance with the Committee for the Purpose of Control and Supervision of Experiments on Animals (CPCSEA) guidelines. For *in vivo* tumorigenic assay, 4T1 cells ( $1 \times 10^6$  cells/animal) were subcutaneously injected into the mammary fat pad of Balb/c mice to develop solid tumor. Animals with solid tumor were randomly distributed into two groups each containing ten animals. One group was treated with vehicle only (0.9% normal saline) whereas, other group was subjected to intraperitoneal injection of RCFE (0.5 mg/kg) starting after 10 days of tumor development and continued until 22 days (4 doses, 72 hr interval). Tumor progression was monitored by measuring the volume of the tumor with vernier calipers on every third day. The tumor volume was calculated by using the formula  $V = 0.5 \times a \times b^2$ , where “a” and “b” indicate length and width diameter, respectively. All animal experiments were conducted in accordance with CPCSEA guidelines and all experimental protocols have been approved by the animal ethics committee of Bose Institute (Ref. No. IAEC/BI/87/2017, dated Dec. 13, 2017) registered with the CPCSEA.

**Fingerprint analysis of *R. Communis* L. fruit extracts.** HPLC and ESI-MS techniques was used to identify the phytochemicals present in the *R. Communis* L. extracts. HPLC fingerprint analysis was performed at  $25 \pm 1$  °C using ethyl acetate fraction of *R. Communis* L. which was dissolved in acetonitrile solvent and filtered through membrane filters (0.45 µm pore size). The sample (20 µL injected volume) was analysed using a Shimadzu system (Kyoto, Japan) equipped with LC-20AT Prominence liquid chromatograph pump, DGU-20A<sub>3</sub> Prominence Degasser, CBM-20A Prominence communications bus module, SPD-20A Prominence UV/VIS detector, LC solution software, and a Rheodyne injector with 100 µL loop.

Separation was achieved using Phenomenex RP C18 column, 250 × 4.6 mm, 5 µm; a gradient mobile phase consisted of water (A) and acetonitrile (B) with a gradient elution program, i.e., 0–40 min, 80–50% B; 40–70 min, 50–0% B; 70–80 min, 0% B; 80–90 min, 0–90% B and 90–100 min 80% B, flow 1 mL/min. The elute was monitored at 210 nm and 254 nm. Mass analysis of the major HPLC peak was recorded on Agilent 6540 Q-TOF LC/MS system.

**Statistical analysis.** Statistical analysis was performed using Graph Pad Prism and data were expressed as mean ± standard deviation (mean ± SD). Results were analyzed either by two-way analysis of variance (two-way ANOVA) or one-way analysis of variance (one-way ANOVA) or Student's t-test as required by the experimental system and difference were considered to be significant at  $p < 0.05$ .

## References

1. Siegel, R. L. *et al.* Colorectal cancer statistics, 2017. *CA: a cancer journal for clinicians* **67**, 177–193 (2017).
2. Tinoco, G., Warsch, S., Glück, S., Avancha, K. & Montero, A. J. Treating breast cancer in the 21st century: emerging biological therapies. *Journal of Cancer* **4**, 117 (2013).
3. Hassan, M., Ansari, J., Spooner, D. & Hussain, S. Chemotherapy for breast cancer. *Oncology reports* **24**, 1121–1131 (2010).
4. Joyce, C. Taxol: search for a cancer drug. *Bioscience* **43**, 133–136 (1993).
5. Noble, R. L. The discovery of the vinca alkaloids—chemotherapeutic agents against cancer. *Biochemistry and cell biology* **68**, 1344–1351 (1990).
6. Xie, S. & Zhou, J. Harnessing Plant Biodiversity for the Discovery of Novel Anticancer Drugs Targeting Microtubules. *Frontiers in plant science* **8** (2017).

7. Canel, C., Moraes, R. M., Dayan, F. E. & Ferreira, D. Podophyllotoxin. *Phytochemistry* **54**, 115–120 (2000).
8. Gordaliza, M., Castro, M. D., Miguel del Corral, J. & Feliciano, A. S. Antitumor properties of podophyllotoxin and related compounds. *Current pharmaceutical design* **6**, 1811–1839 (2000).
9. Moraes, D. F. C., de Mesquita, L. S. S., do Amaral, F. M. M., de Sousa Ribeiro, M. N. & Malik, S. In *Biotechnology and Production of Anti-Cancer Compounds* 121–142 (Springer, 2017).
10. Wang, L. *et al.* Flavonoid baicalein suppresses adhesion, migration and invasion of MDA-MB-231 human breast cancer cells. *Cancer Letters* **297**, 42–48, <https://doi.org/10.1016/j.canlet.2010.04.022> (2010).
11. Yang, P.-M., Tseng, H.-H., Peng, C.-W., Chen, W.-S. & Chiu, S.-J. Dietary flavonoid fisetin targets caspase-3-deficient human breast cancer MCF-7 cells by induction of caspase-7- associated apoptosis and inhibition of autophagy. *International Journal of Oncology* **40**, 469–478, <https://doi.org/10.3892/ijo.2011.1203> (2012).
12. Bachmeier, B. E. *et al.* Curcumin downregulates the inflammatory cytokines CXCL1 and-2 in breast cancer cells via NFκB. *Carcinogenesis* **29**, 779–789 (2007).
13. Hortobagyi, G. The curability of breast cancer: present and future. *European Journal of Cancer Supplements* **1**, 24–34 (2003).
14. Bishop, A. J. *et al.* Prognosis for patients with metastatic breast cancer who achieve a no-evidence-of-disease status after systemic or local therapy. *Cancer* **121**, 4324–4332 (2015).
15. Sajem, A. L. & Gosai, K. Traditional use of medicinal plants by the Jaintia tribes in North. *Journal of Ethnobiology and Ethnomedicine* **2**, 1, <https://doi.org/10.1186/1746-4269-2-33> (2006).
16. Darmanin, S., Wismayer, P. S., Camilleri Podesta, M. T., Micallef, M. J. & Buhagiar, J. A. An extract from *Ricinus communis* L. leaves possesses cytotoxic properties and induces apoptosis in SK-MEL-28 human melanoma cells. *Nat Prod Res* **23**, 561–571, <https://doi.org/10.1080/14786410802228579> (2009).
17. Prakash, E. & Gupta, D. K. *In Vitro* Study of Extracts of *Ricinus communis* Linn on Human Cancer Cell lines. *Journal of Medical Sciences and Public Health* **2**, 15–20 (2014).
18. Jena, J. & Gupta, A. K. *Ricinus Communis* Linn: A Phytopharmacological Review. *International Journal of Pharmacy and Pharmaceutical Sciences* **4**, 25–29 (2012).
19. Shokeen, P., Anand, P., Murali, Y. K. & Tandon, V. Antidiabetic activity of 50% ethanolic extract of *Ricinus communis* and its purified fractions. *Food and Chemical Toxicology* **46**, 3458–3466, <https://doi.org/10.1016/j.fct.2008.08.020> (2008).
20. Gargade, D. G. & Screening, K. of antibacterial activity of *Ricinus communis* L. leaves extracts against *Xanthomonas axonopodis* pv. *punicae*. *International Journal of Advanced Research in Biological Sciences* **2**, 47–51 (2015).
21. Sitton, D. & West, C. A. Casbene: An Anti-Fungal Diterpene Produced In Cell-Free Extract's Of *Ricinus Communis* Seedlings. *Phytochemistry* **14**, 1921–1925 (1957).
22. Upasani, S. M., Kotkar, H. M., Mendki, P. S. & Maheshwari, V. L. Partial characterization and insecticidal properties of *Ricinus communis* L. foliage flavonoids. *Pest Management Science* **599**, 1349–1354, <https://doi.org/10.1002/ps.767> (2003).
23. Attardi, L. D., de Vries, A. & Jacks, T. Activation of the p53-dependent G1 checkpoint response in mouse embryo fibroblasts depends on the specific DNA damage inducer. *Oncogene* **23**, 973–980 (2004).
24. Wachira, S. W. *et al.* Toxicity of six plant extracts and two pyridone alkaloids from *Ricinus communis* against the malaria vector *Anopheles gambiae*. *Parasites & vectors* **7**, 312 (2014).
25. Wafa, G., Amadou, D. & Larbi, K. M. Larvicidal activity, phytochemical composition, and antioxidant properties of different parts of five populations of *Ricinus communis* L. *Industrial Crops and Products* **56**, 43–51 (2014).
26. Singh, P. P. & Chauhan, S. Activity guided isolation of antioxidants from the leaves of *Ricinus communis* L. *Food chemistry* **114**, 1069–1072 (2009).
27. Chin, Y.-W., Balunas, M. J., Chai, H. B. & Kinghorn, A. D. Drug Discovery From Natural Sources. *The AAPS Journal* **8**, E239–E253 (2006).
28. Gordon, M. *et al.* Natural Products in Drug Discovery and Development. *J. Nat. Prod.* **60**, 52–60 (1997).
29. Rates, S. M. K. Plants as source of drugs. *Toxicol* **39**, 603–613 (2001).
30. Leea, H. S., Seob, E. Y., Kangc, N. E. & Kim, W. K. [6]-Gingerol inhibits metastasis of MDA-MB-231 human breast cancer cells. *Journal of Nutritional Biochemistry* **19**, 313–319, <https://doi.org/10.1016/j.jnutbio.2007.05.008> (2008).
31. Krakhmal, N., Zavyalova, M., Denisov, E., Vtorushin, S. & Perelmuter, V. Cancer invasion: patterns and mechanisms. *Acta Naturae (англоязычная версия)* **7** (2015).
32. Choi, Y. H. & Yoo, Y. H. Taxol-induced growth arrest and apoptosis is associated with the upregulation of the Cdk inhibitor, p21WAF1/CIP1, in human breast cancer cells. *Oncology Reports* **28**, 2163–2169, <https://doi.org/10.3892/or.2012.2060> (2012).
33. Nagata, S. Apoptotic DNA Fragmentation. *Experimental Cell Research* **256**, 12–18, <https://doi.org/10.1006/excr.2000.4834> (2000).
34. Leist, M., Single, B., Castoldi, A. F., Kühnle, S. & Nicotera, P. Intracellular Adenosine Triphosphate (ATP) Concentration: A Switch in the Decision Between Apoptosis and Necrosis. *Journal of Experimental Medicine* **185**, 1481–1486 (1997).
35. Elmore, S. Apoptosis: A Review of Programmed Cell Death. *Toxicologic Pathology* **35**, 495–516, <https://doi.org/10.1080/01926230701320337> (2007).
36. Lazebnik, Y. A., KaufmannH, S. H., Desnoyers, S., Poirier, G. G. & Earnshaw, W. C. Cleavage of poly(ADP-ribose) polymerase by a proteinase with properties like ICE. *Nature* **371**, 346–347 (1994).
37. Boulares, A. H. *et al.* Role of Poly(ADP-ribose) Polymerase (PARP) Cleavage in Apoptosis. *The Journal Of Biological Chemistry* **274**, 22932–22940 (1999).
38. Yue, P. & Turkson, J. Targeting STAT3 in cancer: how successful are we? *Expert opinion on investigational drugs* **18**, 45–56 (2009).
39. Pulaski, B. A. & Ostrand-Rosenberg, S. Mouse 4T1 breast tumor model. *Current protocols in immunology* Chapter 20, Unit 20 22, <https://doi.org/10.1002/0471142735.im2002s39> (2001).
40. Rashid, O. M. *et al.* An improved syngeneic orthotopic murine model of human breast cancer progression. *Breast cancer research and treatment* **147**, 501–512 (2014).
41. Rashid, O. M. & Takabe, K. Animal models for exploring the pharmacokinetics of breast cancer therapies. *Expert opinion on drug metabolism & toxicology* **11**, 221–230 (2015).
42. Ferraz, A. C. *et al.* Pharmacological evaluation of ricinine, a central nervous system stimulant isolated from *Ricinus communis*. *Pharmacology Biochemistry and Behavior* **63**, 367–375 (1999).
43. Ohishi, K. *et al.* Ricinine: a pyridone alkaloid from *Ricinus communis* that activates the Wnt signaling pathway through casein kinase 1α. *Bioorganic & medicinal chemistry* **22**, 4597–4601 (2014).
44. Vieira, C. *et al.* Effect of ricinoleic acid in acute and subchronic experimental models of inflammation. *Mediators of inflammation* **9**, 223–228 (2000).
45. Jaganathan, S. K., Supriyanto, E. & Mandal, M. Events associated with apoptotic effect of p-coumaric acid in HCT-15 colon cancer cells. *World Journal of Gastroenterology: WJG* **19**, 7726 (2013).
46. Xuan, H. *et al.* Antitumor activity of Chinese propolis in human breast cancer MCF-7 and MDA-MB-231 cells. *Evidence-Based Complementary and Alternative Medicine* **2014** (2014).
47. Ahmad, N., Feyes, D. K., Agarwal, R., Mukhtar, H. & Nieminen, A.-L. Green tea constituent epigallocatechin-3-gallate and induction of apoptosis and cell cycle arrest in human carcinoma cells. *Journal of the National Cancer Institute* **89**, 1881–1886 (1997).

## Acknowledgements

The study has been performed without funding from any specific agencies. However, RM gratefully acknowledges instrumental facilities provided by Department of Biotechnology, Govt. of India through the projects BT/469/NE/TBP/2013 and BT/410/NE/U-Excel/2013 to his laboratory. MM acknowledges DST-INSPIRE fellowship from Department of Science and Technology for her Ph.D. work.

## Author Contributions

M.M., P.J., K.B. and R.M. designed the experiments. M.M., S.D., R.L.G., R.S., B.G., S.K.S. and D.K.D. performed the experiments. M.M., R.L.G., S.K.S., P.J., K.B. and R.M. analyzed the data. M.M., P.J., K.B. and R.M. wrote and edited the manuscript. All authors approve the manuscript.

## Additional Information

**Supplementary information** accompanies this paper at <https://doi.org/10.1038/s41598-019-50769-x>.

**Competing Interests:** The authors declare no competing interests.

**Publisher's note** Springer Nature remains neutral with regard to jurisdictional claims in published maps and institutional affiliations.



**Open Access** This article is licensed under a Creative Commons Attribution 4.0 International License, which permits use, sharing, adaptation, distribution and reproduction in any medium or format, as long as you give appropriate credit to the original author(s) and the source, provide a link to the Creative Commons license, and indicate if changes were made. The images or other third party material in this article are included in the article's Creative Commons license, unless indicated otherwise in a credit line to the material. If material is not included in the article's Creative Commons license and your intended use is not permitted by statutory regulation or exceeds the permitted use, you will need to obtain permission directly from the copyright holder. To view a copy of this license, visit <http://creativecommons.org/licenses/by/4.0/>.

© The Author(s) 2019



**List of all compounds identified by HR-LCMS analysis from APTE**

# Qualitative Compound Report

<b>Data File</b>	APC-B.d	<b>Sample Name</b>	APC-B
<b>Sample Type</b>	Sample	<b>Position</b>	P1-F7
<b>Instrument Name</b>	Instrument 1	<b>User Name</b>	
<b>Acq Method</b>	30mins_+ESI_10032014.m	<b>Acquired Time</b>	10/8/2018 6:39:45 PM
<b>IRM Calibration Status</b>	Success	<b>DA Method</b>	default.m
<b>Comment</b>			

**Sample Group** Info.  
**Acquisition SW** 6200 series TOF/6500 series  
**Version** Q-TOF B.05.01 (B5125.1)

## Compound Table

Compound Label	RT	Mass	Name	Formula	MFG Formula	DB Formula	DB Diff (ppm)	Hits (DB)
Cpd 1: 2-Amino-3-methyl-1-butanol	0.937	103.0995	2-Amino-3-methyl-1-butanol	C5 H13 N O	C5 H13 N O	C5 H13 N O	2.35	1
Cpd 2: 2-Amino-p-cresol	1.109	123.0681	2-Amino-p-cresol	C7 H9 N O	C7 H9 N O	C7 H9 N O	2.37	7
Cpd 3: PHENYLACETOHYDROXAMIC ACID	1.109	151.0633	PHENYLACETOHYDROXAMIC ACID	C8 H9 N O2	C8 H9 N O2	C8 H9 N O2	0.43	9
Cpd 4: N-Acetylcadaverine	1.17	144.1268	N-Acetylcadaverine	C7 H16 N2 O	C7 H16 N2 O	C7 H16 N2 O	-3.69	2
Cpd 5: Nitrobenzene	1.172	123.0327	Nitrobenzene	C6 H5 N O2	C6 H5 N O2	C6 H5 N O2	-5.77	6
Cpd 6: DL-erythronic acid	1.175	136.0439	DL-erythronic acid	C4 H8 O5	C4 H8 O5	C4 H8 O5	-49.46	5
Cpd 7: S-METHYL-L-THIOCTRULLINE	1.181	205.0991	S-METHYL-L-THIOCTRULLINE	C7 H15 N3 O2 S	C7 H15 N3 O2 S	C7 H15 N3 O2 S	-51.92	1
Cpd 8: Pilocarpine	1.189	208.1214	Pilocarpine	C11 H16 N2 O2	C11 H16 N2 O2	C11 H16 N2 O2	-1.19	1
Cpd 9: TEGASEROD	1.191	301.1889	TEGASEROD	C16 H23 N5 O	C16 H23 N5 O	C16 H23 N5 O	4.47	10
Cpd 10: 1.223	1.223	138.1155						
Cpd 11: 2-Amino-3-methyl-1-butanol	1.347	103.0999	2-Amino-3-methyl-1-butanol	C5 H13 N O	C5 H13 N O	C5 H13 N O	-1.79	1
Cpd 12: 11-amino-undecanoic acid	1.376	201.1725	11-amino-undecanoic acid	C11 H23 N O2	C11 H23 N O2	C11 H23 N O2	1.82	1
Cpd 13: 4-Hydroxybenzyl cyanide	1.475	133.0532	4-Hydroxybenzyl cyanide	C8 H7 N O	C8 H7 N O	C8 H7 N O	-3.18	4
Cpd 14: BENZANTHRONE	1.732	230.0764	BENZANTHRONE	C17 H10 O	C17 H10 O	C17 H10 O	-14.19	4
Cpd 15: trans-trans-Muconic acid	4.426	142.0269	trans-trans-Muconic acid	C6 H6 O4	C6 H6 O4	C6 H6 O4	-2.31	9
Cpd 16: TEGASEROD	4.508	301.1893	TEGASEROD	C16 H23 N5 O	C16 H23 N5 O	C16 H23 N5 O	3.32	10
Cpd 17: trans-trans-Muconic acid	4.631	142.027	trans-trans-Muconic acid	C6 H6 O4	C6 H6 O4	C6 H6 O4	-2.47	9
Cpd 18: 4.893	4.893	164.0591						
Cpd 19: (22S)-1alpha,25-dihydroxy-22-ethoxy-26,27-dimethyl-23,24-tetrahydro-20-epivitamin D3 / (22S)-1alph	5.391	484.3542	(22S)-1alpha,25-dihydroxy-22-ethoxy-26,27-dimethyl-23,24-tetrahydro-20-epivitamin D3 / (22S)-1alph	C31 H48 O4	C31 H48 O4	C31 H48 O4	2.14	9
Cpd 20: Leu Leu Ala	5.817	315.2057	Leu Leu Ala	C15 H29 N3 O4	C15 H29 N3 O4	C15 H29 N3 O4	32.03	10
Cpd 21: EUDESMIC ACID	6.168	212.0672	EUDESMIC ACID	C10 H12 O5	C10 H12 O5	C10 H12 O5	6.19	5
Cpd 22: 5-Hydroxydantrolene	6.418	330.0646	5-Hydroxydantrolene	C14 H10 N4 O6	C14 H10 N4 O6	C14 H10 N4 O6	-13.86	1
Cpd 23: Loganin	6.505	390.1509	Loganin	C17 H26 O10	C17 H26 O10	C17 H26 O10	4.22	10
Cpd 24: 12-amino-dodecanoic acid	6.637	215.1896	12-amino-dodecanoic acid	C12 H25 N O2	C12 H25 N O2	C12 H25 N O2	-4.9	1
Cpd 25: 5-amino-1-[3,4-dihydroxy-5-(hydroxymethyl)oxolan-2-yl]imidazole-4-carboxamide	6.784	258.1093	5-amino-1-[3,4-dihydroxy-5-(hydroxymethyl)oxolan-2-yl]imidazole-4-carboxamide	C9 H14 N4 O5	C9 H14 N4 O5	C9 H14 N4 O5	-49.89	6
Cpd 26: Tyr Pro	7.615	278.1144	Tyr Pro	C14 H18 N2 O4	C14 H18 N2 O4	C14 H18 N2 O4	44.05	3
Cpd 27: 8-CYCLOPENTYLTHEOPHYLLIN	7.842	248.1271	8-CYCLOPENTYLTHEOPHYLLIN	C12 H16 N4 O2	C12 H16 N4 O2	C12 H16 N4 O2	1.06	10
Cpd 28: 3-O-Methylisoproterenol	8.007	225.1364	3-O-Methylisoproterenol	C12 H19 N O3	C12 H19 N O3	C12 H19 N O3	0.42	3
Cpd 29: Acyclovir (8-hydroxy-9-(2-hydroxythoxymethyl)guanine	8.367	239.067	Acyclovir (8-hydroxy-9-(2-hydroxythoxymethyl)guanine	C8 H9 N5 O4	C8 H9 N5 O4	C8 H9 N5 O4	-6.37	4
Cpd 30: Fluconazole	8.482	306.11	Fluconazole	C13 H12 F2 N6 O	C13 H12 F2 N6 O	C13 H12 F2 N6 O	-19.38	10
Cpd 31: p-Nitroglutethimide	8.538	262.1075	p-Nitroglutethimide	C13 H14 N2 O4	C13 H14 N2 O4	C13 H14 N2 O4	-46.36	7
Cpd 32: Arg Asp Asp	8.61	404.1677	Arg Asp Asp	C14 H24 N6 O8	C14 H24 N6 O8	C14 H24 N6 O8	-5.21	10
Cpd 33: Asn His Met	8.85	400.1519	Asn His Met	C15 H24 N6 O5 S	C15 H24 N6 O5 S	C15 H24 N6 O5 S	2.49	10
Cpd 34: BENTAZON	8.953	240.0632	BENTAZON	C10 H12 N2 O3 S	C10 H12 N2 O3 S	C10 H12 N2 O3 S	-26.31	1
Cpd 35: Asn His Met	9.053	400.1519	Asn His Met	C15 H24 N6 O5 S	C15 H24 N6 O5 S	C15 H24 N6 O5 S	2.4	10
Cpd 36: Probenecid	9.095	285.1057	Probenecid	C13 H19 N O4 S	C13 H19 N O4 S	C13 H19 N O4 S	-7.64	10
Cpd 37: Tropicamide	9.348	284.1525	Tropicamide	C17 H20 N2 O2	C17 H20 N2 O2	C17 H20 N2 O2	0.09	3
Cpd 38: Ile Leu Leu	9.466	357.2521	Ile Leu Leu	C18 H35 N3 O4	C18 H35 N3 O4	C18 H35 N3 O4	29.94	8
Cpd 39: Trp Gly Phe	9.581	408.1801	Trp Gly Phe	C22 H24 N4 O4	C22 H24 N4 O4	C22 H24 N4 O4	-0.73	10
Cpd 40: 2-Hydroxydecanedioic acid	9.604	218.1165	2-Hydroxydecanedioic acid	C10 H18 O5	C10 H18 O5	C10 H18 O5	-4.94	10
Cpd 41: 2-Piperidinecarboxamide(PPX)	9.889	232.1586	2-Piperidinecarboxamide(PPX)	C14 H20 N2 O	C14 H20 N2 O	C14 H20 N2 O	-4.55	3

## Qualitative Compound Report

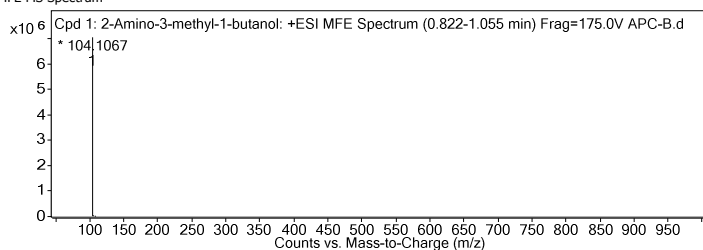
Cpd 42: methyl-10-hydroperoxy-8E,12Z,15Z-octadecatrienoate	9.897	324.2218	methyl-10-hydroperoxy-8E,12Z,15Z-octadecatrienoate	C19 H32 O4	C19 H32 O4	C19 H32 O4	25.56	9
Cpd 43: Ser Tyr Lys	10.356	396.2023	Ser Tyr Lys	C18 H28 N4 O6	C18 H28 N4 O6	C18 H28 N4 O6	-3.57	10
Cpd 44: His Gln Cys	10.692	386.1278	His Gln Cys	C14 H22 N6 O5 S	C14 H22 N6 O5 S	C14 H22 N6 O5 S	24.34	7
Cpd 45: bis(4-fluorophenyl)-Methanone	10.697	218.0541	bis(4-fluorophenyl)-Methanone	C13 H8 F2 O	C13 H8 F2 O	C13 H8 F2 O	0.9	10
Cpd 46: 9-Aminoacridine	11.143	194.085	9-Aminoacridine	C13 H10 N2	C13 H10 N2	C13 H10 N2	-2.91	10
Cpd 47: His Leu	11.151	268.1589	His Leu	C12 H20 N4 O3	C12 H20 N4 O3	C12 H20 N4 O3	-20.13	7
Cpd 48: 2-Hydroxydesmethylimipramine	11.178	282.1742	2-Hydroxydesmethylimipramine	C18 H22 N2 O	C18 H22 N2 O	C18 H22 N2 O	-3.65	5
Cpd 49: 11-dehydro-TXB3	11.739	366.2028	11-dehydro-TXB3	C20 H30 O6	C20 H30 O6	C20 H30 O6	3.81	10
Cpd 50: Idebenone Metabolite (QS-4)	12.135	268.0948	Idebenone Metabolite (QS-4)	C13 H16 O6	C13 H16 O6	C13 H16 O6	-0.25	10
Cpd 51: 9-hydroperoxy-12,13-dihydroxy-10-octadecenoic acid	12.454	346.2368	9-hydroperoxy-12,13-dihydroxy-10-octadecenoic acid	C18 H34 O6	C18 H34 O6	C18 H34 O6	-3.61	10
Cpd 52: 3-Hydroxydodecanedioic acid	12.481	246.1483	3-Hydroxydodecanedioic acid	C12 H22 O5	C12 H22 O5	C12 H22 O5	-6.56	4
Cpd 53: sebacic acid	13.17	202.1216	sebacic acid	C10 H18 O4	C10 H18 O4	C10 H18 O4	-5.35	1
Cpd 54: Lys Cys His	13.218	386.1761	Lys Cys His	C15 H26 N6 O4 S	C15 H26 N6 O4 S	C15 H26 N6 O4 S	-6.51	10
Cpd 55: Lys Lys Thr	13.369	375.2544	Lys Lys Thr	C16 H33 N5 O5	C16 H33 N5 O5	C16 H33 N5 O5	-16.6	3
Cpd 56: 19-hydroxy-PGA2	13.399	350.2086	19-hydroxy-PGA2	C20 H30 O5	C20 H30 O5	C20 H30 O5	2.06	10
Cpd 57: His Lys Cys	13.65	386.1757	His Lys Cys	C15 H26 N6 O4 S	C15 H26 N6 O4 S	C15 H26 N6 O4 S	-5.46	10
Cpd 58: C16 Sphinganine	13.803	273.268	C16 Sphinganine	C16 H35 N O2	C16 H35 N O2	C16 H35 N O2	-4.33	1
Cpd 59: Thromboxane A2	13.902	352.2239	Thromboxane A2	C20 H32 O5	C20 H32 O5	C20 H32 O5	3.05	10
Cpd 60: 14.055	14.055	229.2414						
Cpd 61: Fluprostenol	14.107	458.1969	Fluprostenol	C23 H29 F3 O6	C23 H29 F3 O6	C23 H29 F3 O6	-11.62	6
Cpd 62: 3-Hydroxydodecanedioic acid	14.131	246.1459	3-Hydroxydodecanedioic acid	C12 H22 O5	C12 H22 O5	C12 H22 O5	3.54	3
Cpd 63: o-Methylbenzhydroxyacetic acid	14.217	256.1107	o-Methylbenzhydroxyacetic acid	C16 H16 O3	C16 H16 O3	C16 H16 O3	-3.06	10
Cpd 64: 2beta,7alpha,12alpha-Trihydroxy-3-oxo-5beta-cholan-24-oic Acid	14.247	422.2652	2beta,7alpha,12alpha-Trihydroxy-3-oxo-5beta-cholan-24-oic Acid	C24 H38 O6	C24 H38 O6	C24 H38 O6	3.85	10
Cpd 65: Lys Met His	14.316	414.2074	Lys Met His	C17 H30 N6 O4 S	C17 H30 N6 O4 S	C17 H30 N6 O4 S	-6.06	10
Cpd 66: Cys Lys His	14.423	386.1752	Cys Lys His	C15 H26 N6 O4 S	C15 H26 N6 O4 S	C15 H26 N6 O4 S	-4.04	10
Cpd 67: Azatadine	14.571	290.1735	Azatadine	C20 H22 N2	C20 H22 N2	C20 H22 N2	16.57	4
Cpd 68: Lys Lys Lys	14.636	402.2978	Lys Lys Lys	C18 H38 N6 O4	C18 H38 N6 O4	C18 H38 N6 O4	-5.82	10
Cpd 69: His Lys Met	14.688	414.2071	His Lys Met	C17 H30 N6 O4 S	C17 H30 N6 O4 S	C17 H30 N6 O4 S	-5.25	10
Cpd 70: Dodecanedioic acid	15.001	230.1529	Dodecanedioic acid	C12 H22 O4	C12 H22 O4	C12 H22 O4	-4.58	5
Cpd 71: Asp Pro Arg	15.236	386.1865	Asp Pro Arg	C15 H26 N6 O6	C15 H26 N6 O6	C15 H26 N6 O6	12.74	10
Cpd 72: Tetrahydrocortisol	15.389	366.2407	Tetrahydrocortisol	C21 H34 O5	C21 H34 O5	C21 H34 O5	-0.14	10
Cpd 73: 2,15,16-trihydroxy palmitic acid	15.591	304.2251	2,15,16-trihydroxy palmitic acid	C16 H32 O5	C16 H32 O5	C16 H32 O5	-0.43	10
Cpd 74: Eicosanedioic acid	15.743	342.2887	Eicosanedioic acid	C20 H38 O4	C20 H38 O4	C20 H38 O4	-34.05	6
Cpd 75: Phthalic acid Mono-2-ethylhexyl Ester	15.882	278.1531	Phthalic acid Mono-2-ethylhexyl Ester	C16 H22 O4	C16 H22 O4	C16 H22 O4	-4.72	10
Cpd 76: Phthalic acid Mono-2-ethylhexyl Ester	15.987	278.1532	Phthalic acid Mono-2-ethylhexyl Ester	C16 H22 O4	C16 H22 O4	C16 H22 O4	-5.12	10
Cpd 77: 3beta,7beta-Dihydroxy-12-oxo-5beta-cholan-24-oic Acid	16.085	406.2714	3beta,7beta-Dihydroxy-12-oxo-5beta-cholan-24-oic Acid	C24 H38 O5	C24 H38 O5	C24 H38 O5	1.38	10
Cpd 78: 16.186	16.186	371.9359						
Cpd 79: 3beta,6beta,7alpha-Trihydroxy-5beta-cholan-24-oic Acid	16.369	408.2867	3beta,6beta,7alpha-Trihydroxy-5beta-cholan-24-oic Acid	C24 H40 O5	C24 H40 O5	C24 H40 O5	2.11	10
Cpd 80: Deserpidine	16.952	578.2806	Deserpidine	C32 H38 N2 O8	C32 H38 N2 O8	C32 H38 N2 O8	-30.79	1
Cpd 81: 1,2-di-(5Z,8Z,11Z,14Z,17Z-eicosapentaenoyl)-sn-glycerol	17.286	660.4476	1,2-di-(5Z,8Z,11Z,14Z,17Z-eicosapentaenoyl)-sn-glycerol	C43 H64 O5	C43 H64 O5	C43 H64 O5	42.09	1
Cpd 82: Simvastatin	17.289	418.2704	Simvastatin	C25 H38 O5	C25 H38 O5	C25 H38 O5	3.63	4
Cpd 83: Nanoxynol	17.292	616.4217	Nanoxynol	C33 H60 O10	C33 H60 O10	C33 H60 O10	-4.94	4
Cpd 84: 4-Keto-4'-hydroxyalloxanthin	17.297	594.3772	4-Keto-4'-hydroxyalloxanthin	C40 H50 O4	C40 H50 O4	C40 H50 O4	-10.55	3
Cpd 85: (22S)-1alpha,25-dihydroxy-22-ethoxy-26,27-dimethyl-23,24-tetrahydro-20-epivitamin D3 / (22S)-1alph	17.303	484.342	(22S)-1alpha,25-dihydroxy-22-ethoxy-26,27-dimethyl-23,24-tetrahydro-20-epivitamin D3 / (22S)-1alph	C31 H48 O4	C31 H48 O4	C31 H48 O4	27.33	9

## Qualitative Compound Report

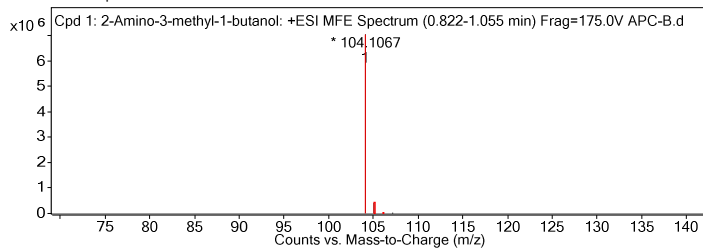
Cpd 86: 24a,24b-Dihomo-9,10-secocholesta-5,7,10(19),24a-tetraen-1alpha,3,25-triol	17.303	440.3156	24a,24b-Dihomo-9,10-secocholesta-5,7,10(19),24a-tetraen-1alpha,3,25-triol	C29 H44 O3	C29 H44 O3	C29 H44 O3	30.43	10
Cpd 87: Isorenieratene/ (Leprotene)	17.303	528.3691	Isorenieratene/ (Leprotene)	C40 H48	C40 H48	C40 H48	12.29	1
Cpd 88: 17.639	17.639	636.3022						
Cpd 89: 14R-hydroxy-11Z-eicosenoic acid	17.813	326.2806	14R-hydroxy-11Z-eicosenoic acid	C20 H38 O3	C20 H38 O3	C20 H38 O3	4.68	10
Cpd 90: 1-Monopalmitin	18.227	330.2778	1-Monopalmitin	C19 H38 O4	C19 H38 O4	C19 H38 O4	-2.41	4
Cpd 91: 18.279	18.279	710.3772						
Cpd 92: 18.635	18.635	710.3744						
Cpd 93: 6alpha-Hydroxy-3-oxo-5beta-cholan-24-oic Acid	18.664	390.2788	6alpha-Hydroxy-3-oxo-5beta-cholan-24-oic Acid	C24 H38 O4	C24 H38 O4	C24 H38 O4	-4.55	10
Cpd 94: 1-octadecanoyl-rac-glycerol	18.756	358.3091	1-octadecanoyl-rac-glycerol	C21 H42 O4	C21 H42 O4	C21 H42 O4	-2.28	7
Cpd 95: (-)-N-(1R-methyl-propyl) arachidonoyl amine	19.171	359.3173	(-)-N-(1R-methyl-propyl) arachidonoyl amine	C24 H41 N O	C24 H41 N O	C24 H41 N O	4.22	7
Cpd 96: 19.948	19.948	662.4501						
Cpd 97: 26.534	26.534	213.911						

Compound Label	Name	m/z	RT	Algorithm	Mass
Cpd 1: 2-Amino-3-methyl-1-butanol	<b>2-Amino-3-methyl-1-butanol</b>	104.1067	0.937	Find by Molecular Feature	103.0995

### MFE MS Spectrum



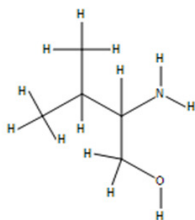
### MFE MS Zoomed Spectrum



### MS Spectrum Peak List

m/z	z	Abund	Formula	Ion
104.1067	1	7053828	C5 H13 N O	(M+H)+
105.1103	1	403343.3	C5 H13 N O	(M+H)+
106.1117	1	23201.39	C5 H13 N O	(M+H)+
107.1145	1	524.39	C5 H13 N O	(M+H)+

### Compound Structure



Compound Label	Name	m/z	RT	Algorithm	Mass
Cpd 2: 2-Amino-p-cresol	<b>2-Amino-p-cresol</b>	124.0758	1.109	Find by Molecular Feature	123.0681

### MFE MS Spectrum

# Qualitative Compound Report

<b>Data File</b>	APC-E.d	<b>Sample Name</b>	APC-E
<b>Sample Type</b>	Sample	<b>Position</b>	P1-F8
<b>Instrument Name</b>	Instrument 1	<b>User Name</b>	
<b>Acq Method</b>	30mins_+ESI_10032014.m	<b>Acquired Time</b>	10/8/2018 7:55:45 PM
<b>IRM Calibration Status</b>	Success	<b>DA Method</b>	default.m
<b>Comment</b>			

**Sample Group** Info.  
**Acquisition SW** 6200 series TOF/6500 series  
**Version** Q-TOF B.05.01 (B5125.1)

## Compound Table

Compound Label	RT	Mass	Name	Formula	MFG Formula	DB Formula	DB Diff (ppm)	Hits (DB)
Cpd 1: 2-Amino-3-methyl-1-butanol	0.893	103.0994	2-Amino-3-methyl-1-butanol	C5 H13 N O	C5 H13 N O	C5 H13 N O	2.73	1
Cpd 2: 2-amino-8-oxo-9,10-epoxy-decanoic acid	0.94	215.1148	2-amino-8-oxo-9,10-epoxy-decanoic acid	C10 H17 N O4	C10 H17 N O4	C10 H17 N O4	4.68	1
Cpd 3: isoamyl nitrite	0.989	117.0786	isoamyl nitrite	C5 H11 N O2	C5 H11 N O2	C5 H11 N O2	3.31	8
Cpd 4: Pyridoxine (Vitamin B6)	1.033	169.0732	Pyridoxine (Vitamin B6)	C8 H11 N O3	C8 H11 N O3	C8 H11 N O3	4.26	4
Cpd 5: 4-Hydroxybenzyl cyanide	1.038	133.0522	4-Hydroxybenzyl cyanide	C8 H7 N O	C8 H7 N O	C8 H7 N O	4.23	4
Cpd 6: 11-amino-undecanoic acid	1.041	201.172	11-amino-undecanoic acid	C11 H23 N O2	C11 H23 N O2	C11 H23 N O2	4.4	1
Cpd 7: pentanamide	1.049	101.0836	pentanamide	C5 H11 N O	C5 H11 N O	C5 H11 N O	4.15	1
Cpd 8: 1.085	1.085	101.1199						
Cpd 9: TUAMINOHEPTANE	1.134	115.1356	TUAMINOHEPTANE	C7 H17 N	C7 H17 N	C7 H17 N	4.76	1
Cpd 10: N-Acetylcadaverine	1.138	144.1278	N-Acetylcadaverine	C7 H16 N2 O	C7 H16 N2 O	C7 H16 N2 O	-10.9	2
Cpd 11: 1.144	1.144	129.1512						
Cpd 12: Leu Leu Ala	1.154	315.2037	Leu Leu Ala	C15 H29 N3 O4	C15 H29 N3 O4	C15 H29 N3 O4	38.29	10
Cpd 13: Leu Leu Ala	4.836	315.204	Leu Leu Ala	C15 H29 N3 O4	C15 H29 N3 O4	C15 H29 N3 O4	37.53	10
Cpd 14: Pyrrole-2-carboxylate	4.88	111.0321	Pyrrole-2-carboxylate	C5 H5 N O2	C5 H5 N O2	C5 H5 N O2	-0.75	8
Cpd 15: Desmethylbetahistine(2-(2-aminoethyl)pyridine)	4.911	122.0842	Desmethylbetahistine(2-(2-aminoethyl)pyridine)	C7 H10 N2	C7 H10 N2	C7 H10 N2	1.3	2
Cpd 16: 5-Hydroxydantrolene	5.039	330.0619	5-Hydroxydantrolene	C14 H10 N4 O6	C14 H10 N4 O6	C14 H10 N4 O6	-5.51	1
Cpd 17: 3-Hydroxy-N-glycyl-2,6-xylidine (3-Hydroxyglycinexylidide)	5.312	194.1044	3-Hydroxy-N-glycyl-2,6-xylidine (3-Hydroxyglycinexylidide)	C10 H14 N2 O2	C10 H14 N2 O2	C10 H14 N2 O2	5.69	1
Cpd 18: DIPHENYLUREA	5.455	212.0949	DIPHENYLUREA	C13 H12 N2 O	C13 H12 N2 O	C13 H12 N2 O	0.43	8
Cpd 19: BENZO[a]PYRENE	5.683	252.0949	BENZO[a]PYRENE	C20 H12	C20 H12	C20 H12	-3.79	10
Cpd 20: Fluconazole	6.179	306.1082	Fluconazole	C13 H12 F2 N6 O	C13 H12 F2 N6 O	C13 H12 F2 N6 O	-13.37	10
Cpd 21: COSMOSIIN	6.274	432.1059	COSMOSIIN	C21 H20 O10	C21 H20 O10	C21 H20 O10	-0.68	4
Cpd 22: Azacitidine	6.372	244.0775	Azacitidine	C8 H12 N4 O5	C8 H12 N4 O5	C8 H12 N4 O5	13.21	10
Cpd 23: Pro Gly Gln	6.426	300.1495	Pro Gly Gln	C12 H20 N4 O5	C12 H20 N4 O5	C12 H20 N4 O5	-20.47	10
Cpd 24: Arg Thr Cys	6.466	378.1678	Arg Thr Cys	C13 H26 N6 O5 S	C13 H26 N6 O5 S	C13 H26 N6 O5 S	1.99	10
Cpd 25: COSMOSIIN	6.517	432.1061	COSMOSIIN	C21 H20 O10	C21 H20 O10	C21 H20 O10	-1.03	4
Cpd 26: Fisetin	6.828	286.0478	Fisetin	C15 H10 O6	C15 H10 O6	C15 H10 O6	-0.28	10
Cpd 27: Rimiterol	6.963	223.1233	Rimiterol	C12 H17 N O3	C12 H17 N O3	C12 H17 N O3	-10.82	3
Cpd 28: Trp Gly Phe	7.013	408.1787	Trp Gly Phe	C22 H24 N4 O4	C22 H24 N4 O4	C22 H24 N4 O4	2.54	10
Cpd 29: epi-4'-hydroxyjasmonic acid	7.285	226.1233	epi-4'-hydroxyjasmonic acid	C12 H18 O4	C12 H18 O4	C12 H18 O4	-12.52	8
Cpd 30: Methylnoradrenaline	7.343	183.0928	Methylnoradrenaline	C9 H13 N O3	C9 H13 N O3	C9 H13 N O3	-17.96	6
Cpd 31: Methyl jasmonate	7.348	224.132	Methyl jasmonate	C13 H20 O3	C13 H20 O3	C13 H20 O3	41.07	8
Cpd 32: Ile Leu Leu	7.401	357.2514	Ile Leu Leu	C18 H35 N3 O4	C18 H35 N3 O4	C18 H35 N3 O4	31.69	8
Cpd 33: Ser Ser	7.579	192.0794	Ser Ser	C6 H12 N2 O5	C6 H12 N2 O5	C6 H12 N2 O5	-24.94	1
Cpd 34: 2,4-octadienal	7.58	124.0915	2,4-octadienal	C8 H12 O	C8 H12 O	C8 H12 O	-21.73	7
Cpd 35: 2E,8E-Undecadiene-4,6-diyenoic acid	7.58	174.0686	2E,8E-Undecadiene-4,6-diyenoic acid	C11 H10 O2	C11 H10 O2	C11 H10 O2	-3.13	4
Cpd 36: 2-METHYL-5,7,8-TRIMETHOXYISOFLAVONE	7.743	326.1162	2-METHYL-5,7,8-TRIMETHOXYISOFLAVONE	C19 H18 O5	C19 H18 O5	C19 H18 O5	-2.43	10
Cpd 37: 4-Hydroxyphenbutolol	7.851	307.2144	4-Hydroxyphenbutolol	C18 H29 N O3	C18 H29 N O3	C18 H29 N O3	1.24	4
Cpd 38: Penbutolol	7.96	291.2194	Penbutolol	C18 H29 N O2	C18 H29 N O2	C18 H29 N O2	1.32	1
Cpd 39: 4,7,10,13-Docosatetraynoic acid	8.144	324.2211	4,7,10,13-Docosatetraynoic acid	C22 H28 O2	C22 H28 O2	C22 H28 O2	-37.48	10
Cpd 40: Mepivacaine	8.272	246.1766	Mepivacaine	C15 H22 N2 O	C15 H22 N2 O	C15 H22 N2 O	-13.86	8
Cpd 41: Primidone	8.32	218.1085	Primidone	C12 H14 N2 O2	C12 H14 N2 O2	C12 H14 N2 O2	-13.66	10
Cpd 42: 6-[5]-ladderane-hexanoic acid	8.935	274.1945	6-[5]-ladderane-hexanoic acid	C18 H26 O2	C18 H26 O2	C18 H26 O2	-4.37	10
Cpd 43: 19(R)-hydroxy-PGB2	8.939	350.2086	19(R)-hydroxy-PGB2	C20 H30 O5	C20 H30 O5	C20 H30 O5	2.09	10

## Qualitative Compound Report

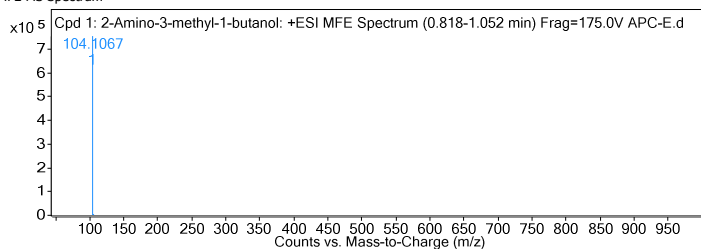
Cpd 44: Neurosporaxanthin beta-D-glucopyranoside	9.375	676.4479	Neurosporaxanthin beta-D-glucopyranoside	C42 H60 O7	C42 H60 O7	C42 H60 O7	-20.68	1
Cpd 45: 5,9-octadecadiynoic acid	9.375	276.2097	5,9-octadecadiynoic acid	C18 H28 O2	C18 H28 O2	C18 H28 O2	-2.65	10
Cpd 46: 15-keto-PGE1	9.376	352.224	15-keto-PGE1	C20 H32 O5	C20 H32 O5	C20 H32 O5	2.73	10
Cpd 47: Diethylpropion	10.005	205.1466	Diethylpropion	C13 H19 N O	C13 H19 N O	C13 H19 N O	0.22	1
Cpd 48: 10.151	10.151	157.1471						
Cpd 49: 10,11-epoxy-3,7,11-trimethyl-2E,6E-tridecadienoic acid	10.295	266.1878	10,11-epoxy-3,7,11-trimethyl-2E,6E-tridecadienoic acid	C16 H26 O3	C16 H26 O3	C16 H26 O3	1.46	10
Cpd 50: His Lys Cys	10.453	386.1742	His Lys Cys	C15 H26 N6 O4 S	C15 H26 N6 O4 S	C15 H26 N6 O4 S	-1.6	10
Cpd 51: 2,3-Diaminopropionic acid	10.456	104.0629	2,3-Diaminopropionic acid	C3 H8 N2 O2	C3 H8 N2 O2	C3 H8 N2 O2	-41.23	1
Cpd 52: 11-Hydroxyandrostosterone	10.721	306.2195	11-Hydroxyandrostosterone	C19 H30 O3	C19 H30 O3	C19 H30 O3	0.14	10
Cpd 53: Androstenedione	10.722	288.209	Androstenedione	C19 H28 O2	C19 H28 O2	C19 H28 O2	-0.41	10
Cpd 54: His Lys Cys	10.905	386.1752	His Lys Cys	C15 H26 N6 O4 S	C15 H26 N6 O4 S	C15 H26 N6 O4 S	-4.08	10
Cpd 55: 2,3-Diaminopropionic acid	10.907	104.0631	2,3-Diaminopropionic acid	C3 H8 N2 O2	C3 H8 N2 O2	C3 H8 N2 O2	-43.22	1
Cpd 56: Sorbaldehyde	10.908	96.0603	Sorbaldehyde	C6 H8 O	C6 H8 O	C6 H8 O	-29.25	2
Cpd 57: Lys Lys Thr	11.219	375.2542	Lys Lys Thr	C16 H33 N5 O5	C16 H33 N5 O5	C16 H33 N5 O5	-16.02	3
Cpd 58: Ranitidine N-oxide	11.744	330.1246	Ranitidine N-oxide	C13 H22 N4 O4 S	C13 H22 N4 O4 S	C13 H22 N4 O4 S	34.94	4
Cpd 59: Asp Pro Arg	11.745	386.1877	Asp Pro Arg	C15 H26 N6 O6	C15 H26 N6 O6	C15 H26 N6 O6	9.64	10
Cpd 60: 2-undecenal	11.804	168.154	2-undecenal	C11 H20 O	C11 H20 O	C11 H20 O	-15.12	3
Cpd 61: Met His Lys	11.835	414.207	Met His Lys	C17 H30 N6 O4 S	C17 H30 N6 O4 S	C17 H30 N6 O4 S	-5.12	10
Cpd 62: 2,4-Diaminobutyric acid	11.84	118.0789	2,4-Diaminobutyric acid	C4 H10 N2 O2	C4 H10 N2 O2	C4 H10 N2 O2	-39.91	1
Cpd 63: 2-undecenal	12.069	168.1537	2-undecenal	C11 H20 O	C11 H20 O	C11 H20 O	-13.38	3
Cpd 64: 12.877	12.877	551.4067						
Cpd 65: 1-Monopalmitin	13.207	330.2795	1-Monopalmitin	C19 H38 O4	C19 H38 O4	C19 H38 O4	-7.58	4
Cpd 66: SPAGLUMIC ACID	13.211	304.0899	SPAGLUMIC ACID	C11 H16 N2 O8	C11 H16 N2 O8	C11 H16 N2 O8	2.58	10
Cpd 67: 13.360	13.36	565.424						
Cpd 68: 13.462	13.462	839.5647						
Cpd 69: C16-OH Sulfatide	13.498	795.5391	C16-OH Sulfatide	C40 H77 N O12 S	C40 H77 N O12 S	C40 H77 N O12 S	-28.22	10
Cpd 70: 1-(6-[5]-ladderane-hexanyl)-2-(8-[3]-ladderane-octanyl)-sn-glycerophosphoethanolamine	13.537	729.531	1-(6-[5]-ladderane-hexanyl)-2-(8-[3]-ladderane-octanyl)-sn-glycerophosphoethanolamine	C43 H72 N O6 P	C43 H72 N O6 P	C43 H72 N O6 P	-29.23	1
Cpd 71: 13.578	13.578	707.488						
Cpd 72: GPEtn(18:0/12:0)[U]	13.623	663.4605	GPEtn(18:0/12:0)[U]	C35 H70 N O8 P	C35 H70 N O8 P	C35 H70 N O8 P	35.22	10
Cpd 73: 13.670	13.67	619.4346						
Cpd 74: 13.719	13.719	558.3809						
Cpd 75: 13.768	13.768	514.3539						
Cpd 76: ((2R)-1alpha,22,25-trihydroxy-26,27-dimethyl-23,24-tetrahydro-24a-homo-20-epivitamin D3 / (22R)-1a	13.817	470.3265	((2R)-1alpha,22,25-trihydroxy-26,27-dimethyl-23,24-tetrahydro-24a-homo-20-epivitamin D3 / (22R)-1a	C30 H46 O4	C30 H46 O4	C30 H46 O4	27.94	8
Cpd 77: 1,2-Dioleoyl phosphatidyl ethanolamine	14.395	743.5444	1,2-Dioleoyl phosphatidyl ethanolamine	C41 H78 N O8 P	C41 H78 N O8 P	C41 H78 N O8 P	2.87	10
Cpd 78: 14.444	14.444	721.5014						
Cpd 79: GPEtn(13:0/18:0)[U]	14.498	677.4749	GPEtn(13:0/18:0)[U]	C36 H72 N O8 P	C36 H72 N O8 P	C36 H72 N O8 P	36.45	6
Cpd 80: 14.554	14.554	633.4498						
Cpd 81: Vitamin D2 glucosiduronate	14.612	572.396	Vitamin D2 glucosiduronate	C34 H52 O7	C34 H52 O7	C34 H52 O7	-43.14	1
Cpd 82: Isorenieratene/ (Leprotene)	14.672	528.3693	Isorenieratene/ (Leprotene)	C40 H48	C40 H48	C40 H48	12.02	1
Cpd 83: ((2S)-1alpha,25-dihydroxy-22-ethoxy-26,27-dimethyl-23,24-tetrahydro-20-epivitamin D3 / (22S)-1alph	14.731	484.342	((2S)-1alpha,25-dihydroxy-22-ethoxy-26,27-dimethyl-23,24-tetrahydro-20-epivitamin D3 / (22S)-1alph	C31 H48 O4	C31 H48 O4	C31 H48 O4	27.34	9
Cpd 84: 1alpha,25-dihydroxy-26,27-dimethyl-22,22,23,23-tetrahydrovitamin D3 / 1alpha,25-dihydroxy-26,27-di	14.778	440.3144	1alpha,25-dihydroxy-26,27-dimethyl-22,22,23,23-tetrahydrovitamin D3 / 1alpha,25-dihydroxy-26,27-di	C29 H44 O3	C29 H44 O3	C29 H44 O3	33.3	6
Cpd 85: Deserpidine	14.853	578.2807	Deserpidine	C32 H38 N2 O8	C32 H38 N2 O8	C32 H38 N2 O8	-30.99	1
Cpd 86: (9Z,12Z)-N-(2-hydroxyethyl)octadeca-9,12-dienamide	15.008	323.2827	(9Z,12Z)-N-(2-hydroxyethyl)octadeca-9,12-dienamide	C20 H37 N O2	C20 H37 N O2	C20 H37 N O2	-0.94	2
Cpd 87: Harderoporphyrin	16.314	608.2655	Harderoporphyrin	C35 H36 N4 O6	C35 H36 N4 O6	C35 H36 N4 O6	-3.35	4

## Qualitative Compound Report

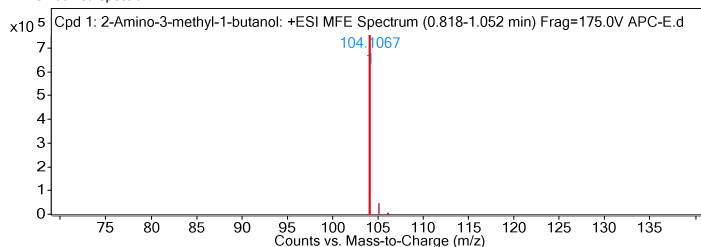
Cpd 88: Dodecaprenyl phosphate-galacturonic acid	16.537	614.3201	Dodecaprenyl phosphate-galacturonic acid	C31 H51 O10 P	C31 H51 O10 P	C31 H51 O10 P	3.12	4
Cpd 89: Harderoporphyrin	16.752	608.2659	Harderoporphyrin	C35 H36 N4 O6	C35 H36 N4 O6	C35 H36 N4 O6	-3.93	5
Cpd 90: 9,12-octadecadienal	16.798	264.2461	9,12-octadecadienal	C18 H32 O	C18 H32 O	C18 H32 O	-3.05	1
Cpd 91: KHAYANTHONE	17.023	570.2882	KHAYANTHONE	C32 H42 O9	C32 H42 O9	C32 H42 O9	-9.37	3
Cpd 92: 17.589	17.589	710.3761						
Cpd 93: DIHYDROGAMBOGIC ACID	18.026	630.3099	DIHYDROGAMBOGIC ACID	C38 H46 O8	C38 H46 O8	C38 H46 O8	14.93	1
Cpd 94: Harderoporphyrinogen	18.098	614.3164	Harderoporphyrinogen	C35 H42 N4 O6	C35 H42 N4 O6	C35 H42 N4 O6	-9.68	4
Cpd 95: 18.318	18.318	710.3738						
Cpd 96: 18.415	18.415	620.3036						
Cpd 97: 26.594	26.594	143.9738						
Cpd 98: 26.603	26.603	102.9476						
Cpd 99: 26.694	26.694	101.1199						
Cpd 100: 26.816	26.816	112.0995						

Compound Label	Name	m/z	RT	Algorithm	Mass
Cpd 1: 2-Amino-3-methyl-1-butanol	<b>2-Amino-3-methyl-1-butanol</b>	104.1067	0.893	Find by Molecular Feature	103.0994

### MFE MS Spectrum



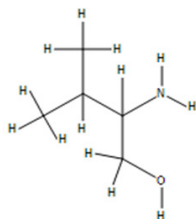
### MFE MS Zoomed Spectrum



### MS Spectrum Peak List

m/z	z	Abund	Formula	Ion
104.1067	1	754742.38	C5 H13 N O	(M+H)+
105.1096	1	43484.29	C5 H13 N O	(M+H)+
106.1111	1	2628.26	C5 H13 N O	(M+H)+

### Compound Structure



Compound Label	Name	m/z	RT	Algorithm	Mass
Cpd 2: 2-amino-8-oxo-9,10-epoxy-decanoic acid	<b>2-amino-8-oxo-9,10-epoxy-decanoic acid</b>	216.1221	0.94	Find by Molecular Feature	215.1148

### MFE MS Spectrum